UNIVERSITY OF OKLAHOMA

GRADUATE COLLEGE

Insights Into the Paleoclimate of the Western Interior Seaway Through the Analysis of Palynomorphs and Petrified Wood from the Short Canyon Member of the Cedar Mountain Formation

A THESIS

SUBMITTED TO THE GRADUATE FACULTY

in partial fulfillment of the requirements for the

Degree of

Master of Science

By

Kaitlyn Murphy
Norman, Oklahoma
2023

Insights Into the Paleoclimate of the Western Interior Seaway Through the Analysis of Palynomorphs and Petrified Wood from the Short Canyon Member of the Cedar Mountain Formation

A THESIS APPROVED FOR THE

SCHOOL OF GEOSCIENCES

BY THE COMMITTEE CONSISTING OF

Dr. Richard Lupia, Chair

Dr. Caitlin Hodges

Dr. Jacqueline Lungmus

ABSTRACT

The Cedar Mountain Formation is a rich source of information on North American megafauna during the Cretaceous, preserving sediments deposited in floodplains related to the Western Interior Seaway. In this thesis, petrified wood, palynomorphs, and wood fragments are identified in the hopes of further building upon what is known about the environment within which Cretaceous megafauna lived. These remains come from the Short Canyon member at the Moore Road Cutoff section and are the first paleobotanical data from this informal member. The petrified wood is identified as *Taxodioxylon albertense*, a cupressaceous conifer with affinities to Sequoioidae, especially *Sequoia* and *Sequoiadendron*. The growth rings of this wood are analyzed and used to interpret water availability in the tree's lifetime, using both seasonal and intraseasonal growth rings. A sediment sample for palynological analysis yielded pollen, spores, cuticle, and wood. Palynomorphs are identified to major group—pteridophytes (e.g., club mosses, ferns, and horsetails), gymnosperms (e.g., cycads, ginkgo, and conifers), or angiosperms (flowering plants)—and abundance counts are made to compare to previous palynological assessments in this formation. These produced pteridophyte-dominated abundances, with roughly equal proportions of angiosperm and gymnosperm pollen. Within the debris in these slides are angiosperm wood fragments. Hardwood features are identified and comparisons to angiosperms previously known from this formation (*Icacinoxylon* and *Paraphyllathoxylon*) are made. From each of these assessments, the paleoenvironment of the Short Canyon member of the Cedar Mountain Formation is interpreted to be a seasonally wet and temperate floodplain.

TABLE OF CONTENTS

CHAPTER 1: BACKGROUND

Introduction:

The Cedar Mountain Formation (CMF) is a dense source of information on the paleoenvironment of the Western Interior Seaway during the Early to "middle" Cretaceous, roughly 126 to 96 Ma. The dinosaurian fauna has been studied since the 1990's, and includes several genera of ankylosaurs, neornithischians, sauropods, and theropods (Kirkland et al., 2016b; Britt et al., 2009; Kirkland et al., 1997). Other vertebrates are also common, such as bony and cartilaginous fish, crocodilians, and lepidosaurian reptiles (Kirkland et al., 2016b; Avrahami et al., 2018; Carpenter and Ishida 2010). Paleofloral data are abundant from the CMF, with diverse microfossil (pollen and spore) floras (Garrison et al., 2007; Joeckel et al., 2020; Tschudy et al., 1984; Carroll 1992), as well as megafossil floras including tree ferns, angiosperms, conifers, and cycads preserved (Dayvault and Hatch 2003, 2007; Thayn and Tidwell 1984; Thayn et al., 1983, 1985; Tidwell and Hebbert 1992; Tidwell and Thayn 1985; see review in Tidwell et al., 2007). The formation is interpreted as a floodplain, with members showing transgression and regression of the Western Interior Seaway and climate changes consistent with global trends (see Kirkland et al., 2016b for example).

Broad Cretaceous:

Overall, the Cretaceous is thought to have had an equable warm and humid climate and is considered a cool greenhouse (Kidder and Worsley 2012; Hay and Floegel 2012). The average global temperature was about 10°C hotter than present, peaking around the Cenomanian-Turonian at ~35°C (see Figure 8 from Hay and Floegel 2012; Hay and Floegel 2012). The latitudinal temperature gradient was weak as well, with smaller changes in temperatures from the equator to the ice-free poles (Hay and Floegel 2012). Reconstructed CO_2 levels for the Cretaceous vary markedly, both between intervals and between studies (see Figure 4 from Quan et al., 2009). In general, CO_2 levels

were significantly higher than today and the middle Cretaceous likely saw values between 500 and 1500ppm, although these levels were decreasing throughout the period (Zhang et al., 2009). Global sea levels fluctuated between roughly present-day levels and up to a maximum of 250m higher than present, with an average between 100-200m higher than present, due to tectonics and changes in seafloor spreading rates (Haq et al., 1987).

There were several short-term episodes of environmental change, where evidence of increasing temperatures and humidity are provided by the rock record. Most events are identified by associations with laminated organic mud deposits, but all are associated with excursions in the $\delta^{13}C$ record (Föllmi 2012). There have been six defined oceanic anoxic events (OAEs), as seen in Table 1 and Figure 1, likely related to excursions into a hothouse climate, with major hothouse episodes also corresponding to large igneous provinces (LIPs) (Kidder and Worsley 2012; Hay and Floegel 2012). There were also arid climate deviations, mostly in the Berriasian and Barremian but also the late Aptian (see Figure 1 from Föllmi 2012).

The Cretaceous was the setting for several major biological radiations and innovations, including the diversification and radiation of angiosperms, sometimes referred to as the Cretaceous Terrestrial Revolution (KTR) or Angiosperm Terrestrial Revolution (ATR; see Figure 2; Lloyd et al., 2008; Benton et al., 2022), as well as the continuation of the placental mammalian radiation (Liu et al., 2017) and several megafauna turnovers, including changes in North American megafauna due to changing continental connections (as discussed in the CMF Fauna section) and the K/Pg mass extinction at the end of the Cretaceous (Tucker et al., 2020; Novacek 1999). The speed and relative recency of angiosperm appearance and evolution in the geologic record was referred to as the "abominable mystery" by Darwin (Friedman 2009). More recently, this abomination has been further elucidated through paleobotanical studies in the rock record and using DNA/RNA analysis

in modern plants (Berendse and Scheffer 2009; Buschiazzo et al., 2012). From the Barremian to the end Cretaceous, angiosperms underwent a radiation that eventually resulted in their dominance over all other flora, reflected both in diversity of form and taxonomic abundance (Knoll 1986; Crane and Lidgard 1989; Lidgard and Crane 1988) although this pattern varies in time and space (Lupia et al., 1999; Nagalingum et al., 2002). Early angiosperms were marginalized and opportunistic, mostly found in disturbed, aquatic, or dry environments (Berendse and Scheffer 2009), but today they account for over 295,000 out of the approximately 370,000 extant plant species (Christenhusz and Byng 2016). The speed and expanse of the radiation has been linked to several possible influences, including, but not limited to, genome downsizing (Simonin and Roddy 2018), novel pollination techniques (Bao et al., 2019), and the combination of a warmer climate that promoted decomposition and an increase in humidity that increased both the relative importance of nutrient availability and the deposition of atmospheric nitrogen (Berendse and Scheffer 2009; Karmakar et al., 2016; Föllmi 2012). The episodic nature of these climate events may have been a driving force in the evolution of higher adaptability of angiosperms to their environments, facilitated by the quick reproductive cycles that genome minimizations provide.

Faunal turnovers are replacements of one biota by another, both taxonomically and morphologically. This is seen in several clades during the Cretaceous but primarily during the Cretaceous Terrestrial Revolution, as in insects, mammals, and perhaps dinosaurs. Insect groups diversified at increased rates during the KTR (Benton et al., 2022). In mammals, the turnover is at its highest rate during the KTR, where the diversity of functional dental types decreases, multituberculates shift to herbivorous diets, and non-multituberculates shift to insectivory, each of which suggests an ecological change related to the diversification of angiosperms and their insect pollinators (Grossnickle and Newman 2016).

The relationship between the mid-Cretaceous dinosaur radiation and the KTR has been passionately debated for several decades (Bakker 1986; Wing and Tiffney 1987; Lloyd et al., 2008). There were dinosaur turnovers related to the Cretaceous; one of these, seen across the J/K boundary, is exhibited as a significant decrease in body size in theropods, as well as decreases in diversity in sauropods and shifts in predominant types of thyreophoran ornithischians as Ankylosauria radiated and Stegosauria declined (Tennant 2016). In the early Late Cretaceous, many herbivorous dinosaur clades arose or diversified, including hadrosaurs, ceratopsians, and ankylosaurs, but this is now thought to be a product of normal diversification rates and not necessarily related to the ATR (Lloyd et al., 2008).

Geological Context:

The Cedar Mountain Formation (CMF) unconformably overlies the Jurassic Morrison Formation and underlies the Cretaceous Naturita Formation (also called the Dakota Sandstone) (Young 1960). Between the Morrison and the Cedar Mountain Formation is an unconformity known as the K-1 unconformity, locally representing between 9 and 20 million years (Kirkland et al., 2016b; Bilbey 1998; Joeckel et al., 2023; Personal communication from Glenn Sharman, 2023). The oldest portions of the formation have recently been dated to the Berriasian or Valanginian, and the youngest to the Cenomanian (Joeckel et al., 2020). The Cedar Mountain Formation formed as a result of the Sevier Orogeny, and local salt tectonics likely played a role in the variety of depths and thicknesses the formation displays as seen in Figure 3 (Kirkland et al., 2016b; Suarez et al., 2021; Currie 1998). The CMF has one informal and five formal members, from oldest to youngest: the Buckhorn Conglomerate, the Yellow Cat Member, the Poison Strip Member, the Ruby Ranch Member, the Short Canyon member, and the Mussentuchit Member (Figure 3).

The Buckhorn Conglomerate is the basal member of the Cedar Mountain Formation and is discontinuous throughout the formation, often channeling into the Morrison Formation. It is largely composed of chert pebble and chert cobble conglomerates, which frequently contain reworked marine fossils from the Paleozoic (Kirkland et al., 2016b). It is thought to be deposited by a complex northeast flowing river system feeding into the Western Interior Seaway (Kirkland et al., 2016b). The Buckhorn Conglomerate often interfingers with beds of iron-stained paleosols (called the Yellow Cat facies of the Buckhorn Conglomerate), indicating a wet climate (Kirkland et al., 2016b).

The next member stratigraphically is the Yellow Cat Member, which consists of drab, variegated, and illitic mudstone, limestone, paleosols, and sandstone lenses. It is divided by the appearance of a calcrete marker bed, with differences between the lower and upper portions including decreases in humidity and changes in fauna, which are interpreted as the result of the initiation of a rain shadow effect (Kirkland et al., 2016b). The lower Yellow Cat is a stacked sequence of root-mottled paleosols with iron oxide nodules, as well as red bed intervals and manganese concretions in the basal contact, suggesting a wet environment. The upper Yellow Cat Member consists of floodplain facies with pedogenic carbonate nodules and ribbon sandstones, thought to represent low sinuosity rivers and lacustrine strata, known as Lake Madsen (Kirkland et al., 2016b). This member has been dated several times, each time resulting in one of two conflicting results. The Yellow Cat Member was tentatively classified as Barremian by carbon isotope analysis (Suarez et al., 2017), although recent literature has proposed a late Berriasian to early Valanginian age (Joeckel et al., 2020; Joeckel et al., 2023). It exhibits $\delta^{13}C$ excursions matching the Weissert event, and a CA-ID-TIMS U-Pb zircon analysis date of 135.10 ± 0.34 Ma (Joeckel et al., 2023). This age interpretation is also supported by the palynology in Joeckel et al., 2020. This would suggest that the unconformity between the Morrison and the Cedar Mountain Formations represents much less time, and the Yellow Cat represents much more time than previously thought. The most recent

study with data taken from not far above the basal contact with the Morrison, yielded a weighted average TIMS date of 126.45 ± 0.08 Ma, which is Barremian (Personal communication from Glenn Sharman, 2023). Hatzell (2015) used the $\delta^{13}C$ of vertebrate herbivore tooth enamel to estimate the $\delta^{13}C$ of plant matter, which was then compared to atmospheric $\delta^{13}C$ estimates to calculate the mean annual precipitation of the member using the equation from Kohn (2010). In the lower Yellow Cat, Hatzell (2015) found a mean precipitation rate of 850 mm/year, and in the upper Yellow Cat an estimate of 455 mm/year.

The Poison Strip Member, originally called the Poison Strip Sandstone, is a complex of well-cemented sandstone beds that indicate deposition in low sinuosity anastomosing and meandering river systems with contemporary interfluvial deposits (Kirkland et al., 2016b). U-Pb dating of carbonates and detrital zircons suggests an Aptian depositional age of 119.4 ± 2.6 Ma (Ludvigson et al., 2010a; Kirkland et al., 2016b). This member produced atypical $\delta^{18}O$ values from poikilotopic calcite cements, but this has been determined to be a result of deep burial diagenesis and the influence of petroleum migration rather than a major climate event (Robertson 2019).

The Ruby Ranch Member is the most widespread and thickest member (see Figure 3). The accommodation space increase was the result of the development of a foreland basin related to the Sevier Orogeny (Kirkland et al., 2016b). It is composed of maroon mudstones with irregular spheres of carbonate nodules. Some deposits are thought to represent a braided, low sinuosity river channel. It is lithologically similar to the Yellow Cat Member, with the main difference being an abundance of carbonate nodules, formed in paleosols and ephemeral ponds under semiarid conditions (Kirkland et al., 2016b). The Ruby Ranch Member is thought to span the Aptian-Albian boundary, based on $\delta^{13}C$ excursions (Kirkland et al., 2016b; Ludvigson 2010). Hatzell (2015) calculated mean annual precipitation at 643 mm/year, a minor increase from the upper Yellow Cat.

The Short Canyon member is an informal member and highly discontinuous in outcrop. It consists of a channel deposit with up to three pebble-to-cobble conglomerates, separated by sandstone and grey-to-black carbonaceous shale (Kirkland et al., 2016b). It is distinguished from the Buckhorn Conglomerate by the inclusion of quartzite clasts, likely derived from the unroofing of the Ordovician Eureka Quartzite (Kirkland et al., 2016b). It is a channel deposit, deposited on the unconformity separating the Ruby Ranch and Mussentuchit Members, and likely partially contemporaneous with the Mussentuchit (Doelling and Kuehne 2013a). In a detrital zircon analysis, a weighted average TIMS date of 103.08 ± 0.05 Ma was found (late Albian; Personal communication from Glenn Sharman, 2023). This age result supports the idea put forward by Doelling and Kuehne (2013a) that the Short Canyon member is closer in age to the overlying Mussentuchit than the underlying Ruby Ranch Member. However, the Short Canyon member is only relatively recently distinguished and thus has not been studied as extensively as the rest of the CMF. The petrified wood studied in this paper originated in the Short Canyon member and is the first contribution to a paleobotanical inventory from this member.

The Mussentuchit Member is composed of grey mudstones with very infrequent carbonate nodules and high organic carbon from plant material and volcanic ash. It is interpreted as a broad coastal plain with a high water level (Tucker et al., 2020). Within this member, there is a base-level rise of brackish groundwater in the lower portion followed by a fall in the upper portion, suggesting transgression and subsequent regression of the Western Interior Seaway (Tucker et al., 2020). The lower portion shows higher humidity levels and plant-rich wetlands, while the upper portion shows fluctuations in humidity (Tucker et al., 2020). It unconformably overlies the Ruby Ranch Member, and conformably overlies the Short Canyon where that member is preserved (Doelling and Kuehne 2013a). Age estimates range from the late Albian to the Cenomanian, based on $^{40}Ar/^{39}Ar$ data,

ranging from 96.7 to 98.5 Ma, and weighted average TIMS dating suggesting 103-99 Ma (Garrison et al., 2007; Personal communication from Glenn Sharman, 2023).

CMF Fauna:

The fauna of the Cedar Mountain Formation has only been studied since the early 90's but has since become well known for having one of the most rich and diverse dinosaur faunas in the world. It has three distinct faunas, interpreted as indicators of the connections between North America and other continents as well as changes in climate (Kirkland et al., 1997). The first of these faunas is the lower "polacanthid" fauna, containing polacanthid ankylosaurs, spatulate-toothed sauropods, basal styracostern "iguanodonts" and large dromaesoaurine dromaeosaurids from the Yellow Cat and Poison Strip Members (Kirkland et al., 2016b). This fauna has genetic links to Europe, suggesting that North America and Europe were connected at the time (Brikiatis 2016). The last land bridge between North America and Europe was likely early in the Barremian, which matches the depositional age of the members containing this fauna (Brikiatis 2016; Kirkland et al., 2016b). The next fauna is the medial "tenontosaurid" fauna, characterized by nodosaurid ankylosaurs, slender-toothed titanosauriform sauropods, and basal iguanodontian tenontosaurids from the Ruby Ranch Member. These taxa are only known from North America during this time period, suggesting that North America had become an isolated continent by this interval (Mannion and Upchurch 2011). The final fauna, the upper "*Eolambia*" fauna, is restricted to the Mussentuchit Member and is dominated by the hadrosaurid iguanodontian *Eolambia*, with some retained taxa from the medial fauna as well as additional taxa that have also been found in Asia (Kirkland et al., 2016b).

CMF Flora:

Dayvault and Hatch (2007) discuss conifer cones from the first few meters above the Buckhorn Conglomerate, although this may represent the Yellow Cat facies of the Buckhorn. The

cones belong to an unknown species of *Araucaria* but were noted as being most similar to *Araucaria mirabilis* and were associated with *Steinerocaulis* sp. and short shoots. In the upper Yellow Cat, a palynological analysis was performed by Joeckel et al. (2020). Of the palynomorphs censused, over half were *Classopollis classoides*, a conifer (genus considered equivalent to *Corollina* in this paper; Traverse 2004). The Yellow Cat sample was devoid of angiosperm pollen and conifer-rich with some spores and algal cysts (Joeckel et al., 2020). Plant fossils in the Ruby Ranch Member are limited to an herbivorous dinosaur coprolite that contained two types of leaf epidermis and possible equisetales remains (Sorscher 2022). Cycads, conifers, and tree ferns have been found in the Poison Strip Member, but many have been poorly preserved, although they often occur as large logs (Kirkland et al., 2016b). Dayvault and Hatch (2005) identified and discussed other finds of these cycads, including a cf. *Bucklandia* sp. cone and trunk, *Monanthesia* sp. with continuous cone structures, *Monanthesia lemonii*, *Cycadoidea medullara,* and *Cycadoidea cleavelandii*, as well as several other specimens that remain unidentified beyond "cycad". These cycads are often found lateral to conifer deposits, but never intermixed. Some of the cycads and conifers contained associated "tiny white blebs" which most likely represent termite-type insects.

In the Mussentuchit, there have been four palynological analyses. The first represents a pteridophyte-dominated palynological profile, with a significant proportion of gymnosperm pollen and a minor proportion of angiosperms (Garrison et al., 2007). Tschudy et al. (1984) noted angiosperm and conifer pollen as well, consisting of tricolpate, bisaccate, and monosulcate pollen, *Classopolis* and few *Liliacidites*, trilete spores, and taxodiaceous pollen. This assemblage appears to have a significant proportion of angiosperms, around equal or slightly less than conifers. Carroll (1992) took samples from several sites, and found one assemblage similar in composition, and therefore age (latest Albian), to Tschudy et al. (1984), and one with far fewer angiosperms that was older. Naeher Stephens (2005) identified several assemblages associated with dinosaur sites. Of

these, many were pteridophyte-dominated both in diversity and in abundance, with low counts of gymnosperms and angiosperms. Notably, conifers were ≤20% of grains in each sample, although the most common taxa within conifers between all sites was *Taxodiaceaepollenites*. These sites can be seen in Figure 5.

Meso- and megafossiliferous botanical matter consists of petrified angiosperm and conifer wood, tree ferns, and possibly leaf fossils. Near Tschudy et al. (1984)'s site, *Tempskya* false trunks were found (Cross et al., 1975 in Tidwell and Hebbert 1992), as well as the angiosperm *Paraphyllanthaxylon utahense* and fronds of *Frenelopsis varians* (Thayne et al., 1983). Other finds include fronds of *Anemia fremontii*, *Tempskya minor*, *T. stichkae*, *T. jonesii*, and *T. wesselii* (Tidwell and Hebbert 1992). At a different site, specimens of *T. jonesii* also occur, along with cycadeoids, the conifers *Mesembrioxylon stokesii* (Thayn and Tidwell 1984) and *Paleopiceoxylon thinosus* (Tidwell and Thayn 1985), and the angiosperms *Paraphyllanthaxylon utahense* and *Icacinoxylon pittiense* (Thayn et al., 1983, 1985, see Tidwell and Hebbert 1992 for summary). An assortment of insect damaged angiosperm leaves was thought to have been collected from the Mussentuchit (Harris and Arens, 2016; Arens and Gleason 2016). However, it is now thought that the strata from which these leaves were collected is related to the deposition of the overlying Naturita Formation, not the Cedar Mountain Formation (Kirkland et al., 2016b).

Lower in the Cedar Mountain Formation, palynology suggests an earlier conifer-dominated ecosystem, with few pteridophytes and no angiosperms. There are some similarities to Morrison flora, especially in the presence and abundance of Araucariaceae (Gee et al., 2014). The lack of pteridophytes suggests a more arid climate. Conifer, cycad, and tree fern megafossils in the Poison Strip Member suggest a transition to a wetter climate, although perhaps the wetness could be somewhat localized in ponds or small bodies of water. Finally, in the Mussentuchit, there are three

palynological interpretations: one pteridophyte-dominated, and the other two gymnosperm-dominated with significant proportions of angiosperms. *Taxodiaceaepollenites hiatus* is frequently described and, although never dominant, it is common and constant in the upper CMF (Garrison et al., 2007).

CMF Paleoenvironment:

Based on the lithology, paleocommunity, and location data, the paleoenvironment of this formation was certainly terrestrial and most likely a floodplain associated with fluvial and lacustrine systems that ultimately fed into the Western Interior Seaway (Young 1960). In general, humidity increases as the Western Interior Seaway transgresses (summarized in Table 2). There is a transition from arid to humid environs between the Morrison Formation and the base of the Cedar Mountain Formation, represented by a reduction in the amount of carbonate nodules (Kirkland et al., 2016b). In the transition from the lower Yellow Cat to the upper Yellow Cat Member, the climate trends arid again (possibly related to a rain shadow effect; see Ludvigson et al., 2015 and Elliot et al., 2007) reflected by an increase in carbonate nodules and the presence of the calcrete layer (Kirkland et al., 2016b). Changes in flora and fauna further support the evidenced changes in hydrology. In these members there are few pteridophytes, which thrive in humid environments (Guo et al., 2003). There is some evidence of a small increase in humidity in the presence of cycads and tree ferns in the Poison Strip Member, which appear laterally to conifer deposits, suggesting ponding or localized wetness. Finally, there is evidence of a transition from arid to humid going from the Ruby Ranch Member into the Mussentuchit, also represented by a decrease in carbonate nodules, possibly a result of the encroachment of the Mowry Sea (Garrison et al., 2007). All evidence suggests a wet and warm climate in the Mussentuchit. These climate trends largely match the general climate trends for the mid-Cretaceous (compare Figure 1 and Table 2).

Overall, there is a trend toward angiosperm domination across the interval, although pteridophytes and conifers (especially taxodiaceous conifers) are present throughout the formation. Below the Mussentuchit, angiosperms are rarely identified, if at all. Instead, there is a dominance of conifers, especially in the Araucariaceae and Cupressaceae families, with numerous algal cysts and few spores (Joeckel et al., 2020). The next significant plant assemblage comes from the Poison Strip Member, containing cycads, conifers, and the tree fern *Tempskya*. Cycads typically grow in tropical to subtropical environments, and *Tempskya* is thought to have a wetland habitat. This suggests a mild transition to a slightly wetter climate, although this is a comparison of different types of data. This "wetter" climate could also be localized, as the cycads and the conifers are found in discrete locations, suggesting ponding and localized wetness. Finally, in the Mussentuchit, pteridophytes or angiosperms dominate, with minor components of conifers and algal cysts. The floral trends in the Cedar Mountain Formation match general climate trends, as well as the timing of the angiosperm radiation.

Purpose:

In this paper, I identify petrified wood from the Short Canyon member of the Cedar Mountain Formation and analyze characteristics that may yield any paleoclimatic data. I also make broad diversity estimates from palynomorphs from the same site and attempt to make any connections to angiosperm or conifer taxa from the wood debris associated with these palynomorphs. With this paleobotanical data, I further reconstruct the paleoenvironment of the western coast of the Western Interior Seaway in the hopes of understanding the habitats and ecosystems the megafauna of the Cedar Mountain Formation inhabited, as well as broadening the current understanding of context of the angiosperm radiation and the Cretaceous Terrestrial Revolution.

CHAPTER 2: METHODOLOGY

Petrified Wood:

During fieldwork in support of NSF EAR-1925896 in June 2021, Marina Suarez, Richard Lupia, and Celina Suarez collected (permit #UT20-005S to M. Suarez) a single piece of petrified wood from a site on Bureau of Land Management property, north of the Moore Road Cutoff, County Road 803, Emery County, Utah (approximate location = 38° 56'N, 111°04'W; black star in Figure 5). The piece was one of several fragments in a linear grouping on the surface of a shoulder of outcrop immediately in front and below an exposure of the Short Canyon Conglomerate. Although not *in situ*, the wood is believed to have originated in the Short Canyon member by proximity, and by association with a large log *in situ* in the Short Canyon about 2 meters north of these fragments. The specimen was catalogued into the Natural History Museum, University of Kansas as C2058. Subsequently, loan #MT02012022 to R. Lupia at the Sam Noble Museum granted permission to destructively sample (for thin sections) this specimen. Additional locality information is available from the Natural History Museum, University of Kansas.

Transverse, tangential, and radial sections of the petrified wood fragment were exposed with an MK 2000 Series brick saw by Ian Taylor and Katie Murphy. Two overlapping sections—aligned by matching growth rings—of the transverse section were chosen from opposite sides of a thin section to extend the growth ring series beyond what would fit on a single slide. The sections were sent to Wagner Petrographic (www.wagnerpetrographic.com) for thin sections and slide preparation including being embedded in blue epoxy. The slides produced were examined under an Olympus BX50 (#9H14094) microscope to identify cellular features and to make a taxonomic identification. Images were captured using a Canon T1i DSLR camera and edited using Adobe Photoshop and Adobe Illustrator. Measurements were performed in Adobe Photoshop and calibrated using a slide micrometer.

Boura, Bamford, and Phillipe's 2021 key of Mesozoic tracheiodoxyl features and the IAWA List of Microscopic Features for Softwood Identification were used to identify cellular features. Phillipe and Bamford's 2008 key to Mesozoic conifer genera was used to make a generic identification. To compare this wood to modern taxa, IAWA features were input into the modern Softwood InsideWood database.

Palynomorphs and Wood Debris:

Also in June 2021, a sediment sample was collected from a lignitic sand at the top of the Short Canyon member, above the highest conglomerate in a section adjacent to the Moore Road Cutoff (approximate location = 38° 56' N, 111° 04'W; County Road 803, Emery County, Utah). The sediment was sent to Global Geolab, Ltd (https://www.globalgeolab.com/) in Alberta, Canada for processing. Standard palynological processing techniques (e.g., Dohrer 1980; Traverse 2007) were used, including hydrochloric and hydrofluoric acid digestion as well as oxidation; to separate organic fraction, the residue was sieved with a 10 μm sieve, then a 5 μm sieve. The resulting palynomorphs were prepared on slides using a fixing medium and were not stained. This resulted in six slides: one kerogen slide from residue before sieving, three 10 μm slides prepared from residue before the final sieve, and two 5 μm slides.

Over 150 palynomorphs were censused from the two slides sieved at 5 μm from the Moore Road Cutoff section and were identified to three broad categories: pteridophyte spores, gymnosperm pollen, and angiosperm pollen. Palynomorphs were identified to major categories—pteridophyte spores, gymnosperm pollen, and angiosperm pollen —by comparison to known palynomorphs from the Cedar Mountain Formation (Naeher Stephens 2005; Garrison et al., 2007; Tschudy et al., 1984; Carroll 1992). Wood fragments were examined from each of the six slides and

features were identified by comparison to the IAWA List of Microscopic Features for Hardwood Identification and the IAWA List of Microscopic Features for Softwood Identification.

CHAPTER 3: RESULTS AND DESCRIPTION

Petrified Wood Description:

Sample: C2058 (Table 3)

Site: Moore Road Cutoff (Figures 4 and 5)

Formation: Short Canyon member of the Cedar Mountain Formation

Age: Albian

Preservation: Throughout the tracheiodoxyl, preservation is generally good. It is highly resiniferous. There is evidence of crushing, especially when viewing in the transverse section, as well as a section that may represent rot along one of the growth rings.

Transverse Section, Plate I: Tracheids are rounded polygonal in earlywood and compressed rectangles with significantly thickened cell walls in latewood (Plate I, Figures 1-4). Axial parenchyma is abundant and diffuse, with occasional zonation. The parenchymatous cells are resiniferous, smaller than their surrounding tracheids, and tend to be rectangular in shape (Plate I, Figure 1). Growth rings are abrupt and distinct, type D under Creber and Chaloner's 1984 categorization, with latewood only 2-4 cells deep. Between the two transverse slides there are a total of 29 growth rings represented in C2058, with 16 on TR1 and 13 on TR2. When duplicate rings are removed, 21 growth rings remain. Of these, 11 exhibit characteristics of seasonal growth rings, while the other 10 exhibit characteristics of intraseasonal growth rings, such as limited cell wall thickening, inconsistencies across the growth ring (i.e., latewood terminates laterally or conjoins with a seasonal growth ring), and a less distinct transition from latewood back into earlywood (Plate I, Figures 1-3). There are two crushed zones where additional growth rings might be concealed. Rot may be preserved along one of the growth rings. There are 1-(4)-7 tracheids between ray cells. Medullary

rays are resiniferous, and globules of resin are often associated with crossfield pits within tracheids (Plate I, Figures 5 and 6). There are no resin canals, normal or traumatic.

Tangential Section, Plate II: Rays are very tall, measuring 1-(13)-65 cells and 56-(398)-1599 μm tall (Plate II, Figure 1). Rays are predominantly uniseriate (89%), with frequent local biseriation between 10-30% of the total ray length, and rare multiseriation. Single biseriate pairs have an opposite arrangement, while larger areas are alternately arranged. Axial parenchyma is frequent and distinct. Intertracheary pits are commonly seen in radial walls, but not in tangential walls (Plate II, Figures 2 and 3).

Radial Section, Plates III-VI: Intertracheary pits are primarily uniseriate, although roughly 25% are biseriate with both isolated pairs and larger areas of opposite biseriation present. Isolated pairs are primarily oppositely arranged but can be sub-alternate to alternate. Pitting is mostly abietinean (intertracheary pits are round and distant from neighboring pits) but is often mixed. The bordered pits measure 13-(19)-25 μm in diameter and are unornamented. They are round, with a length to width ratio averaging 0.96. Crassulae are present but infrequent. Individual ray parenchyma cells are 72-(137)-270 μm wide and 14-(23)-36 μm tall. Ray end walls are thin and smooth, but slightly thicker in the transverse walls. Ray-tracheid crossfields contain 1-2 (up to 3) primarily taxodioid but frequently cupressoid pits at a roughly 45° angle. The shape of the crossfield pitting can also vary locally to glyptostroboid or podocarpoid.

An elliptical boring of indeterminate origin is present, measuring 2957 μm wide by 2487 μm tall. It is not filled with fragmented wood cell frass, although a few latewood tracheids are present. It contains black masses that are suspected to be frass composed of fungal hyphae. The rest of the borehole is filled with a yellow substance that is assumed to be amber. There appears to be a large,

branched object in the middle, although that is suspected to be an artifact of sap flow. There are fungal hyphae in the tracheids surrounding the boring, measuring 0.8-1.5 μm in diameter.

Palynology Results:

On slide 5 μm-02, 193 palynomorphs were identified. Of these, 169 were spores (87.5%), 10 were angiosperm pollen (5.2%), and 14 were gymnosperm pollen (7.3%). On slide 5 μm-03, 158 palynomorphs were identified. Of these, 139 (88.0%) were spores, 9 (5.7%) were gymnosperm, and 10 (6.3%) were angiosperm (See Table 4 and Figure 6).

Wood Fragment Descriptions:

IAWA Hardwood Features: 10 or 11, 19, 20, 21, 22, 32, 37, 60(?), 61, 62; **Plate VII**

IAWA Softwood Features: 44, 56, 58, 61, 93(?); **Plate VIII**

Within the organic material in the palynology slides, several wood fragments with identifiable features were found. Because of the diversity of these features, they likely do not represent a single species. Despite this, some connections to a clade could be made from any features that are exclusive to a group. An example of this is cupressaceous crossfield pitting, which is limited to three groups of conifers: Cupressaceae (except for *Thuja*), Podocarpaceae, and Taxaceae (Esteban et al., 2023). The majority of the fragments with identifiable features are attributable to angiosperms. These features are frequently difficult to accurately diagnose, as they are disconnected from any context and many features of angiosperm wood share forms with other features, such as scalariform perforation plates and scalariform intervessel pitting. Because of the size of the fragments, these features are found in isolation and no positive connections can be made between them.

In the angiosperm wood fragments, many of the identifiable fragments are fibers characterized by narrow diameters (11-31 μm) and scattered unbordered to half bordered pits. There are fibers with simple to minutely bordered pits less than 3 μm in diameter (IAWA HW 61), as in

Figures 1, 2, and 6 of Plate VII. There are also fibers with distinctly bordered pits (IAWA HW 62) or half-bordered pits, as in Figures 3 and 4 of Plate VII. Other features of fibers found include warty layers (Plate VII, Figure 6) and textured parenchyma end walls (Plate VII, Figure 5).

Intervessel pitting is seen frequently. The most common type of intervessel pits are round and alternate, with aperture shape varying from circular to ovular to slits (Plate VII, Figures 9, 12 and 13; IAWA HW 22). There are also scalariform to opposite intervessel pits with slits, although this is infrequent (Plate VII, Figure 11; IAWA HW 20, 21). Another common form of intervessel pits are long scalariform sections, as seen in Plate VI, Figures 7 and 8 (IAWA HW 20). These are frequently sequential laterally, suggesting vessels are commonly continuous (IAWA HW 10 or 11). For example, Plate VI, Figure 8 has 5 sequential columns of scalariform pitting, suggesting at least 6 sequential vessels and possibly up to 10.

Some scalariform features have reticulate features integrated and could be considered opposite intervessel pitting, a relatively infrequent angiosperm trait, as in Plate VII, Figures 11, 15, and 16 (IAWA HW 21). Some of these, namely Plate VII, Figures 14-16, may represent perforation plates instead. The perforation plates that were identified are regularly reticulate (Plate VII, Figure 17), scalariform to reticulate (Plate VII, Figures 15 and 16), scalariform to regularly reticulate (Plate VII, Figure 18), reticulate (Plate VII, Figures 22 and 13), and foraminate (Plate VII, Figure 24; all are IAWA HW 19). Potential vessel-ray pits are seen in Plate VII, Figures 19-21. These have reduced borders and a vertical palisade arrangement, presenting as long oval pits parallel to the long axis of the cell, as opposed to perpendicular in the scalariform features (IAWA HW 32).

In the gymnosperm (and origin unknown) fragments (Plate VIII), helical thickenings, bordered pits, and potential crossfield pits are shown. Many fragments are found with spiral

thickening, as in Plate VIII, Figure 1. In many of these fragments, the neighboring cells have spiral thickenings as well (IAWA HW 37; SW 61).

One feature that is commonly seen but difficult to identify are xylem cells with evenly spaced lines perpendicular to the cell walls that continue into the next cell, as in Plate VIII, Figures 2, 3, and 8. These occur as thick walls that are even in length or thicken as the wall of the fiber is approached. In Plate VIII, Figure 8, they appear more like crassulae in that they are rounded at the ends, past the cell wall. These frequently contain pits that are evenly distributed within these walls. The pits are similar to a few features, including bordered pits with distinct crassulae and cupressaceous crossfield pits. It is likely that the features identified here represent both. The diameters of these cells are in the range of large fibers or small tracheids (around 30 μm) and may represent vascular or vasicentric tracheids (IAWA HW 60). If these fragments represent angiosperms, a likely origin of these features are vasicentric tracheids with annular or horizontal spiral thickenings and large bordered pits, as seen in Figure 8 of Parameswaran and Vidal Gomes (1981). In gymnosperms, these most likely represent cupressoid crossfield pitting (Plate VIII, Figures 2, 3, 8, and potentially 5; IAWA SW 93).

Plate VIII, Figures 4-7 and 9-16 represent the variety of bordered pits. These likely have gymnosperm origins. The most common bordered pits are roughly circular with round apertures and are generally distant from neighboring bordered pits (represented by Plate VIII, Figure 4; IAWA SW 44). One variation is ovular and large with oval apertures, as seen in Figures 11 and 13. There are also small ovular bordered pits with round apertures, as seen in Figure 12. These are seen very close to, but not touching, neighboring pits, which is unusual for bordered pits with this length to width ratio. There are also round bordered pits with elliptical apertures, as in Figures 6 and 7. Some bordered pits may have torus extensions, as seen in Figures 9 and 10, or have visible tori (Figures 10, 14, and 15; IAWA SW 56, 58). Biseriate bordered pits are rarely seen, as in Figure 16.

CHAPTER 4: IDENTIFICATION

Petrified Wood:

Phillipe and Bamford (2008) created a key to genera of Mesozoic fossil woods. Based on their key and the following characters, C2058 is identified as *Sequoioxylon* or *Taxodioxylon*. The key features used include:

> "1') all rays uniseriate, except for some local biseriation
>
> 4') radial pits never scalariform
>
> 7') axial parenchyma present or absent, neither particularly associated with the ray nor inflated
>
> 9') all ray cell walls thin and smooth, unpitted
>
> 10') abietinean pitting on radial wall of tracheids (i.e., with more than 90% of the pits separate, rounded, while biseriate or pluriseriate always clearly opposite; some contiguous pits are possible, and even locally short chains; rosette-like clusters of 3-4 pits sometimes encountered)"

Key characters 1-10 qualify this specimen as belonging to Phillipe and Bamford's (2008) Group C. Within this group, the key characters are:

> "Group C, 1') in the earlywood oopores to taxodioid oculipores (i.e., with the aperture wider than one margin), usually arranged irregularly
>
> Group C, 2') earlywood cross-fields with oculipores
>
> Group C, 5") both resin canals and spiral thickenings absent
>
> Group C, 6') crossfield pits mostly less than four, spaced, sometimes ordered in rows

Group C, 7) oculipores in earlywood cross-fields of the taxodioid type, i.e., with a tangential aperture, wider than one margin (but not bordered oopores or circopores), usually more or less horizontal."

These characters delimit two very similar genera: *Sequoioxylon* and *Taxodioxylon*. To evaluate between them, the original and emended diagnoses were closely evaluated. The diagnosis for *Sequoioxylon* is as follows:

> "Annual rings strongly developed; contrast between spring and summer wood very marked. Resin canals wholly traumatic and in one or both directions. Wood rays with a few oculipores or oopores on the lateral tracheid-field; other walls either smooth or sparingly pitted. Resinous wood parenchyma present, diffuse, sometimes confined to the summer wood. Tracheids with one to several rows of bordered pits separated by bars of Sanio, and when in more than one row, opposite" (originally from Torrey 1923, taken from Phillipe and Bamford 2008).

The diagnosis for *Taxodioxylon* is as follows:

> "Wood of conifer; rays uniseriate; no resin canals; axial parenchyma; cross-field pits not contiguous; no tertiary thickenings; tracheids with 1–2 rows of radial pits, pits distant; ray cells parallel-sided, no more that 4–5 times longer than high; axial parenchyma cells parallel-sided, isolated or paired, 1–3 times higher than broad, as wide or wider than the tracheids when seen from the ray cell side" (translated from Hartig 1848 in Phillipe and Bamford 2008).

Based on the lack of traumatic resin canals, which serves as the primary difference between these genera, this specimen of wood most closely matches *Taxodioxylon*. An in-depth discussion of the two genera is presented in the *Taxodioxylon* discussion section.

The species of this wood is interpreted as *Taxodioxylon albertense* (Penhallow) Shimakura. The primary characteristics that lend themselves to this identification are the number and diversity of crossfields and the height of the rays. This species was described twice, first by Penhallow (1908) as *Sequoia albertensis*, then emended by Shimakura (1937) to update the generic and specific epithets to *Taxodioxylon albertense* and to add the presence of traumatic resin canals. Shimakura noted frequent traumatic resin canals and rare single resin canals, both of which were absent in Penhallow's original description. This wood most closely matches Penhallow's description and comparisons to both the original and emended descriptions are provided in Table 6.

This specimen differs from Shimakura's description by the presence of alternate tracheid pitting (which is absent in Shimakura's description), 1-3 crossfield pits (as opposed to 1-2), an abrupt transition from early- to latewood (as opposed to gradual), and the absence of traumatic resin canals. Alternate bordered pit pairs are infrequent enough in this wood that it could be considered unnoteworthy. In fact, a pair of bordered pits that would have been described as alternate or sub-opposite in this thesis is present in Plate 27, Figure 5 of Kim's 2005 review of Shimakura's wood. The same logic applies to the presence of three crossfield pits. These are rare, with this specimen containing at most five to six crossfields bearing three pits. In Shimakura (1940), another specimen is analyzed, noting that three crossfield pits in a crossfield does occur. In C2058, growth rings are extremely shallow, and in Shimakura's wood the growth rings are much deeper (see Kim 2005, Plate 27, Figure 1). While latewood depth can be a taxonomic character, it also varies with wood height within the tree and climate, as discussed in the Growth Rings section. The final incongruous trait is the presence of traumatic resin canals, which have already been shown to be a variable trait in *T. albertense*. Traumatic resin canals form in response to trauma. If the tree that produced this wood didn't experience any events that would trigger their formation in the period recorded by this

specific section of wood, there would not be any traumatic resin canals. These lifetime variations are also discussed in Shimakura's 1937 paper.

Differential diagnosis:

Other species considered included were *Taxodioxylon taxodii*, *T. cryptomeriodes*, *T. drumhellerense, T. multiseriatum, T. gypsaceum,* and *T. cabullensis*. These were considered because they are also present in North America. Many of these were easily eliminated due to a few features in this sample, but primarily the notably tall rays. Only one other *Taxodioxylon* species came close to the maximum ray height exhibited, and while ray height is typically not a major distinguishing character, the degree of difference between the tallest ray in this wood and most other species of *Taxodioxylon* is significant. Results are summarized in Table 6.

Taxodioxylon cabullensis Ríos-Santos & Cevallos-Ferriz has smaller bordered pits with oval openings and notches, lacks crassulae, has shorter rays with different cell shapes, and 1-9 primarily cupressoid crossfield pits (Ríos-Santos and Cevallos Ferriz 2019). In contrast, the bordered pits in this specimen are unornamented and large, the rays are up to 3 times taller, and the crossfields primarily contain 1-2 taxodioid pits per crossfield. The parenchymatous cells are also both shorter and thicker than in this specimen. This species is definitely cupressaceous, although I personally would not classify it as *Sequoioxylon/Taxodioxylon* because the crossfield pits are predominantly cupressoid. *Taxodioxylon cryptomerioides* Schoenfield has rare crassulae and rays 1-20 cells tall (Ramanujam 1972). The crossfield pits have thicker borders and are arranged vertically or diagonally. In C2058, crassulae are common, the rays are much taller, and the crossfield pits have thinner borders and are arranged horizontally. The latewood is also much deeper in *T. cryptomerioides*. *Taxodioxylon taxodii* Gothan has up to triseriate bordered pits, trabeculae, rays 3-55 cells tall, and 2-6 pits per crossfield (Ramanujam and Stewart 1969). The bordered pits in C2058 are never triseriate, it

lacks trabeculae, has rays much taller, and primarily 1-2 crossfield pits per crossfield. *Taxodioxylon gypsaceum* (Göppert) Kräusel has up to triseriate bordered pits, zonate axial parenchyma, rays that are 2-35 cells tall, and has 2-8 taxodioid pits per crossfield as well as tangential tracheid pitting. This differs from C2058, which has uni- to biseriate bordered pits, diffuse as opposed to zonate axial parenchyma, rays that are 2-70 cells tall, and primarily 1-2 taxodioid pits per crossfield (Ramanujam and Stewart 1969). *Taxodioxylon drumhellerense* Ramanujam & Stewart has rays 2-25 cells tall, triangular intercellular spaces between rays and tracheids, spiral checking, and 1-6 crossfield pits that can be taxodioid or glyptostroboid (Ramanujam and Stewart 1969). C2058 has rays 2-70 cells tall, no intercellular spaces, and 1-3 crossfield pits. *Taxodioxylon multiseriatum* Ramanujam has smaller bordered pits, spool-shaped or bar-like trabeculae, rays 2-70 cells tall (but primarily 12-25), and zones with multiseriate rays (Ramanujam 1972). *Taxodioxylon multiseriatum* is the species that is the most similar to C2058 after *T. albertense*. It differs primarily in the presence of trabeculae and the frequency of multiseriate rays, and perhaps the frequency of axial parenchyma. C2058 has occasional multiseriate rays, although infrequent, that are never tetraseriate.

Although these species of *Taxodioxylon* occur in North America and share many features, none of them match this specimen as closely as *T. albertense*.

Wood Fragments:

Some of the features of the angiosperm wood fragments are reflected in angiosperms previously discovered in the Cedar Mountain Formation. The first angiosperm wood found in this formation, *Paraphyllanthoxylon utahense*, has oppositely arranged bordered intervascular pits with slit-like apertures (Plate VII, Figures 9, 10, 12, and 13; Thayne et al., 1983). The vessel-ray pits in this species also match the ones seen in Plate VII, Figures 19-21. The rays in this species might also account for the beaded features seen in Plate VII, Figure 6. If that is the case, the minutely bordered

pits seen in fibers are likely attributable to this species as well. Simple to minutely bordered fiber-tracheid pits are not included in the paper describing *P. utahense,* although this feature is marked as present on the InsideWood database.

Icacinoxylon pittiense, another angiosperm from the CMF, likely accounts for another portion of the wood fragments (Thayn et al., 1985). Fiber-tracheids in this species have bordered pits that match the ones found in fibers in the fragments (Plate VII, Figures 3 and 4). In the intervessel pits, there are widely spaced scalariform to opposite slightly bordered pits with large apertures (Plate VII, Figures 11 and 14-16). The perforation plates are elongated scalariform plates 4 to 30+ bars long (Plate VII, Figures 7 and 8 potentially).

In the gymnosperm features, it seems unlikely that many, if any, are associated with *Taxodioxylon*. The cupressaceous crossfield pits may be from wood in this genus, although if they were it would be unusual to not find taxodioid crossfield pits as well (Plate VIII, Figures 3, 5, and 8). The number and arrangement would be consistent with many species of *Taxodioxylon*, including the type specimen of *T. albertense* (Penhallow 1908). The typical bordered pits (Plate VIII, Figure 4) match the abietinean pits in *T. albertense*. In the other gymnosperms found in this formation, *Mesembrioxylon stokesii* has bordered pits that resemble those in Plate VIII, Figures 9 and 10 (compare Plate VIII, Figure 10 to Figure 2 in Thayn and Tidwell 1984). *Paleopiceoxylon thinosus* does not seem to account for any of the gymnosperm features seen in these fragments (Tidwell and Thayn 1985).

Many features cannot be accounted for in the taxa already known from the Cedar Mountain Formation. The species known from the CMF do not have helical thickenings, nor do they have large bordered pits. There are also no irregularly reticulate, regularly reticulate, or foraminate perforation plates seen in these angiosperm species.

CHAPTER 5: DISCUSSION

Petrified Wood Assignment:

Taxodioxylon:

The difference between *Taxodioxylon* and *Sequoioxylon* is not well defined. *Taxodioxylon* was first described by Gothan (1905) and was redefined by Hartig (1948) to include all Sequoieae, Taxodieae, and Cunninghamieae (Akkemik 2019). Taxodiaceous wood was discussed by Tian et al., 2018, who suggested that *Sequoioxylon* should be defined by the presence of traumatic resin canals, while the lack of traumatic resin canals indicated *Taxodioxylon*. Ironically, Penhallow first named the species *Sequoia albertensis* when his specimen did not have traumatic resin canals while Shimakura renamed the species *Taxodioxylon albertense* based on his specimen that did have traumatic resin canals. This is completely antithetical to the modern definitions. Because of this variability not only within the two genera but within this species, in this thesis I consider the genera to be functionally synonymous.

Other Findings of Taxodioxylon:

There have been two other samples of *Taxodioxylon* found in the United States from the Cretaceous, both near the border to other countries. The first of these comes from Falcon-Lang (2003), from the Campanian Two Medicine Formation in Montana. It is only identified as a *Cupressinoxylon/Taxodioxylon* type by the author, although it seems like the *Cupressinoxylon* species it most closely resembles has an incomplete description and the specimen itself shares more features with both *Taxodioxylon cryptomerioides* and *T. drumhellerense*. This specimen will be discussed further in the growth ring discussion. The other Cretaceous *Taxodioxylon* from the United States comes from Ibrahim (2015), where petrified wood from the Campanian Aguja Formation is identified to genus.

Other Cretaceous North American *Taxodioxylon* that were identified to species include the type specimen of *Taxodioxylon albertense* from the Maastrichtian in Alberta (Penhallow 1908), *T. cryptomerioides* and *T. multiseriatum* from the Campanian in Alberta (Ramanujam 1972), *T. drumhellerense, T. gypsaceum, T. multiseriatum*, and *T. taxodii* from the Maastrichtian in Alberta (Ramanujam and Stewart 1969b and c), and *T. cabullensis* from the Santonian to the late Maastrichtian (Rios-Santos and Cevallos-Ferriz 2019). A map of the distribution of these findings is available in Figure 7.

Taxodioxylon albertense:

There are eight reported samples of *Taxodioxylon albertense*, spread between Asia, Europe, and North America. Of these, seven are from the late Cretaceous and the eighth, the largest *in situ* petrified tree trunk in Europe, is from the Miocene (Zouros 2021; see Table 7), making the specimen described in this thesis the oldest known specimen of *T. albertense*. The type specimen is the only other specimen of the species from North America.

This specimen most closely resembles the specimen described in Kim et al. (2002). Most notably, the growth ring characteristics are extremely similar. The other specimens of *T. albertense* I have been able to find in plates and figures typically have deeper latewood with a much more gradual transition, as well as less variation in crossfield pitting morphology. As discussed previously, these two characters can be fairly variable between individuals in the species and may have been influenced by climate.

Modern Affinities:

The family Taxodiaceae has recently been dissolved as there is no phylogenetic difference between taxa in Taxodiaceae and the rest of Cupressaceae, with the exception of the genus *Sciadopitys*, which has been removed from Cupressaceae altogether (Román-Jordán et al., 2017). Taxodiaceae contained ten modern genera: *Athrotaxus*, *Cunninghamia*, *Cryptomeria*, *Sciadopitys, Sequoia,*

Sequoiadendron, Metasequoia, Glyptostrobus, Taiwania, and *Taxodium* (Román-Jordán et al., 2017). The taxodiaceous genera that were not removed from Cupressaceae have been regrouped into five subfamilies: Athrotaxidoideae, Cunninghamioideae, Sequoioideae, Taiwanioideae, and Taxodioideae.

Taxodioxylon albertense has mild affinities to *Metasequoia* and *Glyptostrobus*, the two of which can be difficult to distinguish based on wood characteristics, but it most closely resembles *Sequoiadendron* and *Sequoia*, two of the three genera in Sequoioideae. *Sequoiadendron* is represented by one extant species, *S. giganteum*, and one extinct species, *S. chaneyi. S. giganteum* is also known as the giant redwood and is paleoendemic to the Sierra Nevada of California (Dodd and DeSilva 2016). They are the most massive trees on earth, meaning they have a high volume of wood, and reach heights of 50m. *Sequoiadendron* also has some of the tallest rays in modern Cupressaceae, up to 30 cells high (Román-Jordán et al., 2017). In Penhallow's original diagnosis, he notes the striking affinity of *Taxodioxylon albertense* to *Sequoia semperviens. S. semperviens*, in contrast to *Sequoiadendron*, is the tallest tree on earth, growing over 100m tall. It is limited to a narrow flood-prone zone near the California coast (Noss 2000). These two tree species are very closely related, so much so that it is thought that *Sequoia* is a result of reticulate evolution between *Sequoiadendron* and *Metasequoia* (Yang et al., 2012). They also have very similar water needs, as both require massive amounts of water to sustain their mass, and both are adapted to wildfire survival (Noss 2000). The water needs of *Sequoiadendron* may be a driving force in their reduction of range, as it has been linked to increasing aridity in the past two million years (Dodd and DeSilva 2016).

The features of C2058 that most closely resemble *Sequoiadendron* include the arrangement, number, and shape of the crossfield pits. There are typically 1-2 cupressaceous or taxodioid crossfield pits per crossfield, arranged horizontally or randomly. It differs from C2058 in the presence of a warty layer in the axial tracheids, the presence of traumatic resin canals, tangential

pitting in latewood, trabeculae, and transverse end walls of axial parenchyma can be irregularly thickened or nodular (Román-Jordán et al., 2017).

Spatial Interpretations:

There are common themes in the Cretaceous North American *Taxodioxylon*, both temporally and spatially: most come from the late Cretaceous, either Campanian or Maastrichtian, and are on the western coast of the Western Interior Seaway, as in Figure 7 and Table 5. One outlier was found in Nova Scotia, from the Valanginian-Hauterivian, which is earliest Cretaceous (Falcon-Lang et al., 2007). This wood, another outlier, comes from the Albian, which is very late Early Cretaceous.

These themes are consistent with the continental connections shown in the changing faunas. The single *Taxodioxylon* from the Early Cretaceous is found in northeastern North America, towards Europe. The lower "polacanthid" fauna, which comes from the Barremian Yellow Cat Member of the Cedar Mountain Formation, is related to European taxa. The rest of the *Taxodioxylon* are in western North America, towards Asia. The upper "*Eolambia*" fauna from the Albian-Cenomanian Mussentuchit Member, has several taxa that have also been found in Asia. Additionally, most of the other specimens of *Taxodioxylon albertense* from the Cretaceous are found in Asia, specifically Japan, South Korea, and the Sakhalin Oblast of Russia (Table 7). These are all in eastern Asia, close to North America. It is important to note, however, that this correlation may instead be the product of a bias in deposition. Cretaceous deposits in North America are widespread in the west but are much smaller and may be less heavily studied in the east (Barton et al., 2003). Additional findings of *Taxodioxylon* from eastern North America would help confirm or deny this trend.

Some of the petrified woods identified in the Cedar Mountain Formation (or close relatives) are described alongside *Taxodioxylon albertense* in Asian localities, most notably in Shimakura (1937) with *Mesembrioxylon stokesi*, but also in Nishida (1986) with *Tempskya sp.* as discussed in Tidwell and

Hebbert (1992). This suggests a similar climate and further corroborates the identification of this wood, as well as contributes to the evidence for the Asian-North American land bridge.

Features of the wood:

Growth ring series:

Growth ring series in extant woods are often calibrated to regional records of water regime, temperature, and extreme weather events in order to understand how these environmental factors affect specific characteristics of growth in that tree species (i.e., Therrell et al., 2020). These can have such accuracy that specific tracheids can be linked to the day they were formed (Therrell et al., 2020). Different species of trees can react very differently to the same stimuli, even between those that are thought to be very closely related (Carroll et al., 2014). One example of this is a comparison of growth ring formation over 1,500+ years between *Sequoia sempervirens* and *Sequoiadendron giganteum*, the two modern species to which *Taxodioxylon albertense* has the most affinities. *S. giganteum* has complacent growth rings, meaning rings with little annual variation. These rings are generally very consistent in terms of depth, with deviations being linked to major climate events. In contrast, *S. sempervirens* has rings that can be discontinuous, or merge with neighboring rings, or even missing. They are also complacent rings, however, and are largely insensitive to climate (Carroll et al., 2014).

The inconsistencies between these two modern species are inconvenient for understanding the growth ring behavior of *Taxodioxylon albertense*, but the consistency is incredibly useful: complacent rings. Any variability in growth ring depth in species with complacent rings indicates large scale changes in weather and environment. There is evidence of complacent rings in C2058. Many of the growth rings are relatively consistently spaced and concentric, with roughly equal latewood depth (see Figure 8 for the growth ring series). The growth ring intervals that deviate from this pattern likely indicate intense climate variation. This can be approached in two ways: depth of

seasonal growth rings and placement of intraseasonal growth rings within these seasonal patterns. In this specimen, seasonal growth rings deviate from the average annual depth by getting deeper, reflecting an increase in water availability. This is especially evident in the gaps between the seasonal growth rings 1 and 3, and 11 and 15, which are two to three times as deep as the typical growth rings, such as growth rings 3-11 (Figure 8b, orange box indicates dry/typical years, green boxes indicate wet years).

Similar to seasonal growth rings, intraseasonal growth rings indicate major climate events, usually droughts. Location within the seasonal growth rings can be indicative of different processes, but all are ultimately related to a decrease in water availability. Intraseasonal growth rings late in a growth ring can indicate an increase in water availability after the late season drying, stalling the formation of late wood and a temporary return to early wood. Intraseasonal growth rings early in the growth ring can indicate a drought interrupting the growing season (Therrell et al., 2020; Copenheaver et al., 2017). Either way, there is a decrease in water availability, whether typical or atypical for the season, followed by an increase in water availability. Intraseasonal rings can occur due to any number of circumstances, including physical damage (such as insects, fire, disease, wind), drought, floods, and competition within a forest, but are thought to primarily be related to climate and are almost exclusive climate-related in species with complacent rings (Edmonson 2010). In this wood, there are climate instability intervals within a larger stable climate, or at the very least a climate that is stable at the resolution of complacent rings.

Latewood depth is a variable trait in *Taxodioxylon* (compare Falcon-Lang and Cantrill 2000 to Falcon-Lang 2003). Some specimens of *Taxodioxylon* form more latewood than other species in the same environment, as seen in Falcon-Lang and Cantrill (2000). Others, including C2058, form extremely shallow latewood. Earlywood and latewood have different functions throughout the

growing season. Latewood stores more water and uptakes less, more concerned with making it through the winter than immediate use and growth, while earlywood starts grows using that stored water (Palakit et al., 2012). Latewood depth can be a factor of climate, genetics, or just the wood's original height position within the tree (the higher up in the tree, the less latewood forms), but this all varies with species (Creber and Chaloner 1984). This is best shown in tropical areas with stable yearlong climates where trees frequently do not form growth rings because there is not a significant trigger to slow the production of the vascular cambium, such as fewer hours of sunlight per day, temperature decreases, decreases in water availability, or the loss of leaves (Detienne 1989). In some trees, growth rings weaken but do not completely disappear. The same species of tree in different climates will form differing amounts of latewood. In *Pinus sylvestris*, boreal trees form much deeper latewood than trees in warm and dry Mediterranean biomes (Camarero et al., 2021). The same paper also suggests that trees in warm and dry Mediterranean climates (as opposed to cold and dry Mediterranean climates) could be valuable drought proxies.

Another sample of *Taxodioxylon* with similar growth ring characteristics comes from Falcon-Lang 2003, where a sample with exclusively intraseasonal growth rings was found. This sample was compared to conifers in East Africa that exhibited very similar growth ring patterns. The climate was described as having a relatively stable temperature variability and most growth rings are formed in response to erratic water availability (Falcon-Lang 2003).

There are several discrete pieces of knowledge to gain from the growth ring series in this sample. First, a climate record lasting approximately 14 years. Second, major climate patterns in the spacing of seasonal growth rings and the location of intraseasonal growth rings, indication frequent variation in water availability. Finally, there are similarities to a climate that is seasonally wet and has

low annual temperature variability in the depth of the latewood, frequency of intraseasonal rings, and in the affinities to *Sequoiadendron* and *Sequoia*.

Insect boring:

Insect borings are a common feature in petrified wood (i.e., Deng et al., 2022). Many of these are preserved as series of tunnels in petrified logs. In this wood, there is not nearly as much context, only a single view of a boring. Most wood borings are insect created, usually beetles, moths, or wasps (United States Department of Agriculture, 2011). This boring is captured in the radial plane, travelling tangentially. This could be one tunnel in a series of parallel tunnels, as in Mikuláš et al. (2020).

There is no sign of wound response in the cells surrounding the borehole, nor any traumatic resin canals in any part of the tracheiodoxyl. Additionally, xylophages tend to preferentially inhabit dead or dying wood, which this specimen likely was based on the rot present (Feller 2002). There are also fungal hyphae beginning decomposition in the body of the wood, but only in the area surrounding the borehole. These signs point to postmortem boring, although they do not preclude the possibility that the boring occurred antemortem. Traumatic resin canals are formed by the vascular cambium and do not form in wood that has ceased differentiation (Nagy et al., 2000). The creator of the boring traveled into wood that had already been formed, and if traumatic resin canals were going to form, they could have formed in wood that was not preserved here. Many woodboring insects have associated fungi, and the fungal hyphae present could have been seeded by these insects before tree death (Skelton et al., 2019).

To investigate the timing of the boring in the tree's life, the contents of the boring can be used: the frass and the sap. An oddity of this boring is the lack of wood frass. Many insect borings are full of sawdust-like frass (see Genise and Hazeldine 1995). In this boring, there are a few cells

that may represent wood cells, but not nearly as many as is expected (Plate IV, Figure 3). Frass is present, though primarily composed of fragments of fungal hyphae (Plate IV, Figure 2). The near absence of wood cells suggests that they were cleared out, perhaps by the borer. Some insects do this in nesting activity, such as carpenter ants, as their goal for boring into the wood is shelter as opposed to nutrition (Akre and Hansen 1990). The secondary hyphal frass could have been left by an insect similar to a springtail, of which there are some species that feed primarily on fungal hyphae (Castaño-Meneses et al., 2017). Not only would this show that there was an abundance of decomposition occurring around this tree, but it would also support the idea of a postmortem boring.

The collembola-type frass has two or three centers of gravity: one at 90°, another at around 225°, and a minor one at 270°. This suggests a slow flow of sap and movement while sap was flowing. The first center of gravity, being perpendicular to the tracheids, signals the wood lying flat on the ground. This mass is more continuous with the body of the resin, suggesting it was deposited while the sap was still flowing. The second center of gravity, depositing frass at 225°, is bordered to the right by laminations in the resin, suggesting the sap was flowing around it. This suggests the left deposit was cemented first and may have occurred while this piece was in life position. The angle would suggest this piece came from a branch, or from a tree that grew diagonally, as if on a slope.

Palynology:

The results of the palynological samples in this thesis fit well into what is expected in the Cedar Mountain Formation. The palynology from Joeckel et al. (2020) in the upper Yellow Cat Member shows a gymnosperm-dominated environment, with less than 2% pteridophyte spores and no angiosperms. This is exactly what would be expected in such an arid climate, especially when the ATR is still picking up steam and angiosperms are not yet widespread. The next palynological study

in this formation is from this thesis, in the upper portion of the Short Canyon member. The results from this thesis contain a large percentage of pteridophytes (88%) while the remainder are split approximately equally between angiosperm and gymnosperm pollen. If the wood fragments in these same slides are from *Paraphyllanthoxylon* and *Icacinoxylon*, a wetter and more tropical climate would be expected, as is reflected in the dominance of pteridophytes. In the Mussentuchit Member, presented here without regard to stratigraphic position within this member, the palynological abundances vary greatly. In each of the samples from the CMF (excluding Garrison et al., 2007 due to a lack of direct abundance data), there is an increase in angiosperms, with abundance percentages ranging from 7% to 47% (Naeher Stephens 2005 site RRQ and Tschudy et al., 1984 respectively). The Albian and Cenomanian saw incredibly fast diversification of angiosperms, so it is not unreasonable for angiosperm abundance to increase so rapidly in this time frame (see Figure 4).

An unusual result from the palynology slides is the relative proportions of angiosperm to gymnosperm wood and pollen. With the amount of angiosperm wood fragments, more angiosperm pollen might be expected. The angiosperm fragments show affinities to Lauraceae, which produces pollen that is rarely preserved due to a thin exine (Herendeen et al., 1993). This could account for the relative lack of angiosperm pollen in samples from the Cedar Mountain Formation, as nearly all of the fragments have features that are attributable to Lauraceae. Additionally, the heartwood of angiosperms is resistant to decay, which may lead to a positive preservation bias in the wood fragments.

Wood Fragments:

Many of the angiosperm wood fragments found can be referred to at least two genera: *Icacinoxylon* and *Paraphyllanthaxylon*. These woods have been previously found in the Mussentuchit Member of this formation, specifically *Paraphyllanthaxylon utahense* and *Icacinoxylon pittiense*, the two of

which account for many, but not all, of the angiosperm features described. In other species of these genera, a few of the remaining features can be seen.

The group of species of *Paraphyllanthaxylon* that resemble *P. utahense* show similarities to several families, including Lauraceae, Elaeocarpaceae, Anacardiaceae, and Burseraceae (Herendeen 1991). Species of *Paraphyllanthoxylon* that resemble *P. utahense* most closely include *P. marylandense, P. idahoense, P. alabamense*, and *P. capense*, all from the Cretaceous (Herendeen 1991). *P. marylandense* is suspected to be most closely related to Lauraceae, a basal angiosperm family whose extant taxa include bay laurels, cinnamon trees, and avocados, all of which occur in tropical and warm temperate regions. In the fossil record, these have been found all over the world (Jud et al., 2017). It is often considered to be a basal angiosperm. *Icacinoxylon* is the name for fossilized woods resembling the family Icacinaceae, the white pear family (Thayne et al., 1985). These are primarily tropical taxa.

P. marylandense has many similarities to the yet-unidentified features seen in these wood fragments, including the helical thickenings and occasional large bordered pits in tracheary elements, and other features that have already been assigned to *P. utahense* in these fragments, such as the alternate and long scalariform intervascular pitting (see Plate II, Figure 7 and Plate IV, Figures 5 & 6 in Herendeen 1991 for comparison).

Further confirmation of these generic identifications—*Paraphyllanthoxylon* and *Icacinoxylon*—would indicate a slightly warmer climate than is presently interpreted on the basis of palynological data and conifer wood. These fragments are only tentatively assigned to these taxa because the characteristics seen in these fragments are individually consistent with the generic circumscription. With increased prospecting, larger fragments may reveal combinations of characters that are incompatible with these genera, revealing the presence of other angiosperm taxa. If these taxa can be proven to be present in the Short Canyon member, a wetter habitat would be interpreted

somewhere in this landscape, similar to the localization of cycads and gymnosperms in the Poison Strip Member. This could also be an effect of the different stratigraphic levels that the samples studied in this thesis represent, as the palynodebris samples were taken from the top of the Short Canyon while the petrified wood is assumed to have come from the bottom of the Short Canyon. When compared to the interpreted water regimes of the Short Canyon member and the Mussentuchit Member, the paleoenvironment of these wood fragments fit well within the increasing humidity of the Short Canyon into the Mussentuchit. This, along with the unpublished detrital zircon age of the Short Canyon member, supports the concept from Doelling and Kuehne (2013a), suggesting that the deposition of the Short Canyon member is more closely related to the deposition of the overlying Mussentuchit Member than it is to the underlying Ruby Ranch Member.

CHAPTER 6: CONCLUSIONS

The Cedar Mountain Formation contains a wealth of information on the changing climate of the late Early Cretaceous. In this thesis, the first paleobotanical evidence from the Short Canyon member of this formation is identified and climatic interpretations are made. From a specimen of *Taxodioxylon albertense*, there is clear evidence of a fluctuating climate. From the wood itself, there is evidence of decomposers in the forms of an insect boring and infiltrating fungal hyphae. There is evidence of a temperate climate in the depth of latewood, and of periodic droughts in the frequency and location of intraseasonal growth rings. Lastly, the presence of this species, which was also found in Korea and Japan, further supports the idea of a land bridge between Alaska and Asia at this time that is suggested by the fauna of the Cedar Mountain Formation.

The features of this specimen of *T. albertense* and the modern taxa to which this wood has the closest affinities are linked to climates in which rainfall is heavily seasonal and there are minimal annual temperature variations. This interpretation of the Short Canyon member climate is congruent with what is inferred about the Cedar Mountain Formation from other climate proxies (e.g., sedimentology, isotopes), and indicates an intermediate climate phase in the transition from the semi-arid Ruby Ranch Member into the very humid Mussentuchit Member, further supporting an increase in water availability with the encroachment of the Western Interior Seaway (See Table 2).

Although the analyzed petrified wood revealed a conifer, angiosperm wood fragments are found as microfossils in the dispersed palynological record. These fragments appear to represent a woody angiosperm population with affinities to Lauraceae, and further build upon the preexisting evidence of angiosperms in this formation. Additionally, many of these fragments cannot be ascribed to previously known angiosperms from this formation. The palynology and wood

fragments from higher in the Short Canyon suggest an increasing humidity within this member, further strengthening the genetic linkage between the Short Canyon and the Mussentuchit.

Future work:

The Short Canyon member occupies a transitional interval between the Ruby Ranch and Mussentuchit Members. As such, further paleobotanical research, including palynology and macrofossils, could reveal new data to tease apart climate, vegetational and perhaps faunal changes observed between the units. The presence of large in situ logs (Figure 4b) indicate that longer time series of annual rings are available to document rainfall/season variability. That such logs are possibly common across available outcrops is suggested by posts on Reddit, potentially in the Short Canyon member (chasingthewhiteroom 2021). Additional material may provide for the identification of large angiosperm trees in the Short Canyon member at the end of the Albian.

TABLES AND FIGURES

Table 1

Major Climate Events of the Cretaceous

EVENT	OAE	DATE
Weissert Event	--	Valanginian
Faraoni Event	--	Latest Hauterivian
Taxy Event	--	Latest Barremian-earliest Aptian
Selli Event	OAE1a	Early Aptian
Fallot Event	--	Early late Albian
Paquier Event	OAE1b	Late Aptian-early Albian
Toolebuc Event	OAE1c	Late Albian
Breistoffer Event	OAE1d	Albian-Cenomanian
Bonarelli Event	OAE2	Cenomanian-Turonian
--	OAE3	Late Coniacian

Note: Information compiled from Freymueller (2019), Jenkyns (2010), Föllmi (2012), and Leckie et al., (2002).

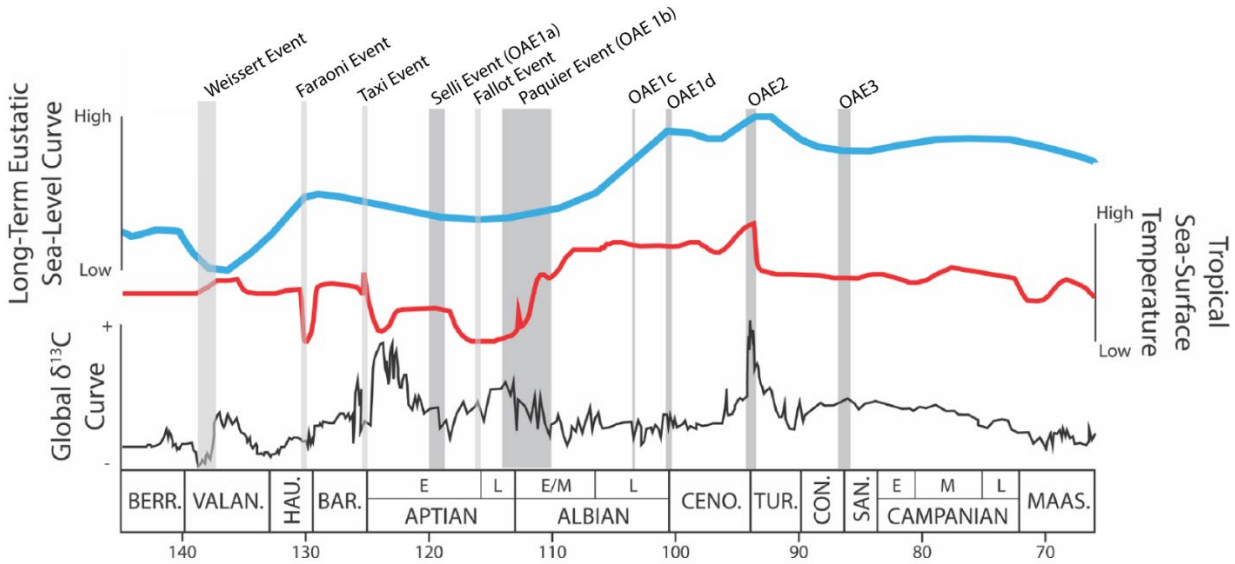

Figure 1: Cretaceous OAEs and climate events compared to a long term eustatic sea level curve, tropical sea-surface temperatures, and $\delta^{13}C$ curves. Adapted from Figure 1 from Freymueller et al. (2019).

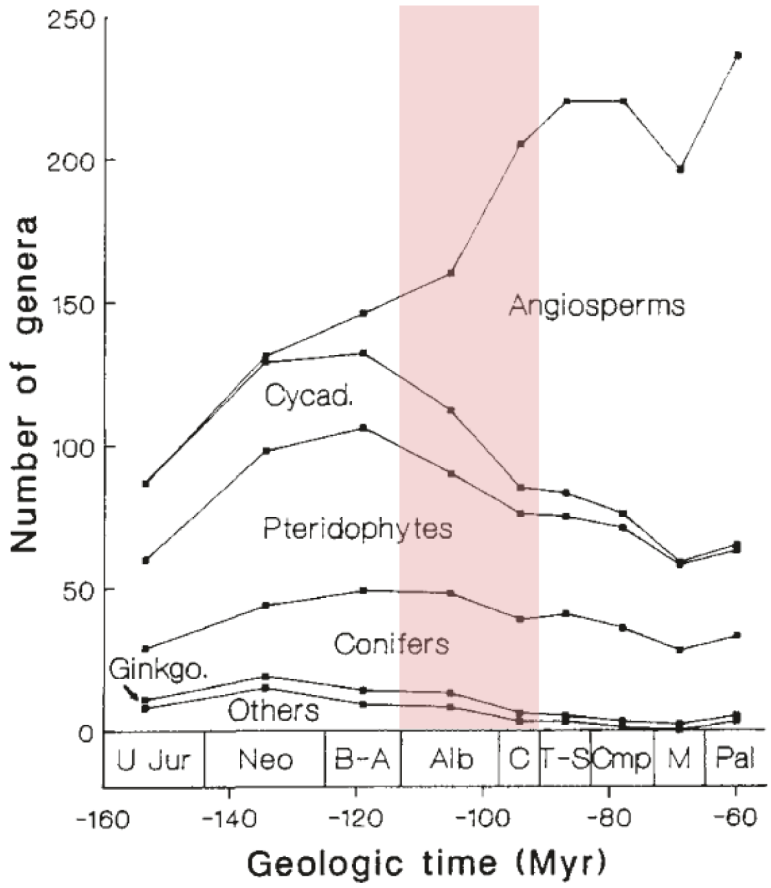

Figure 2: Angiosperm diversification as measured by number of genera per group. The Albian and Cenomanian are highlighted in pink. Adapted from Figure 1 from Lidgard and Crane (1988).

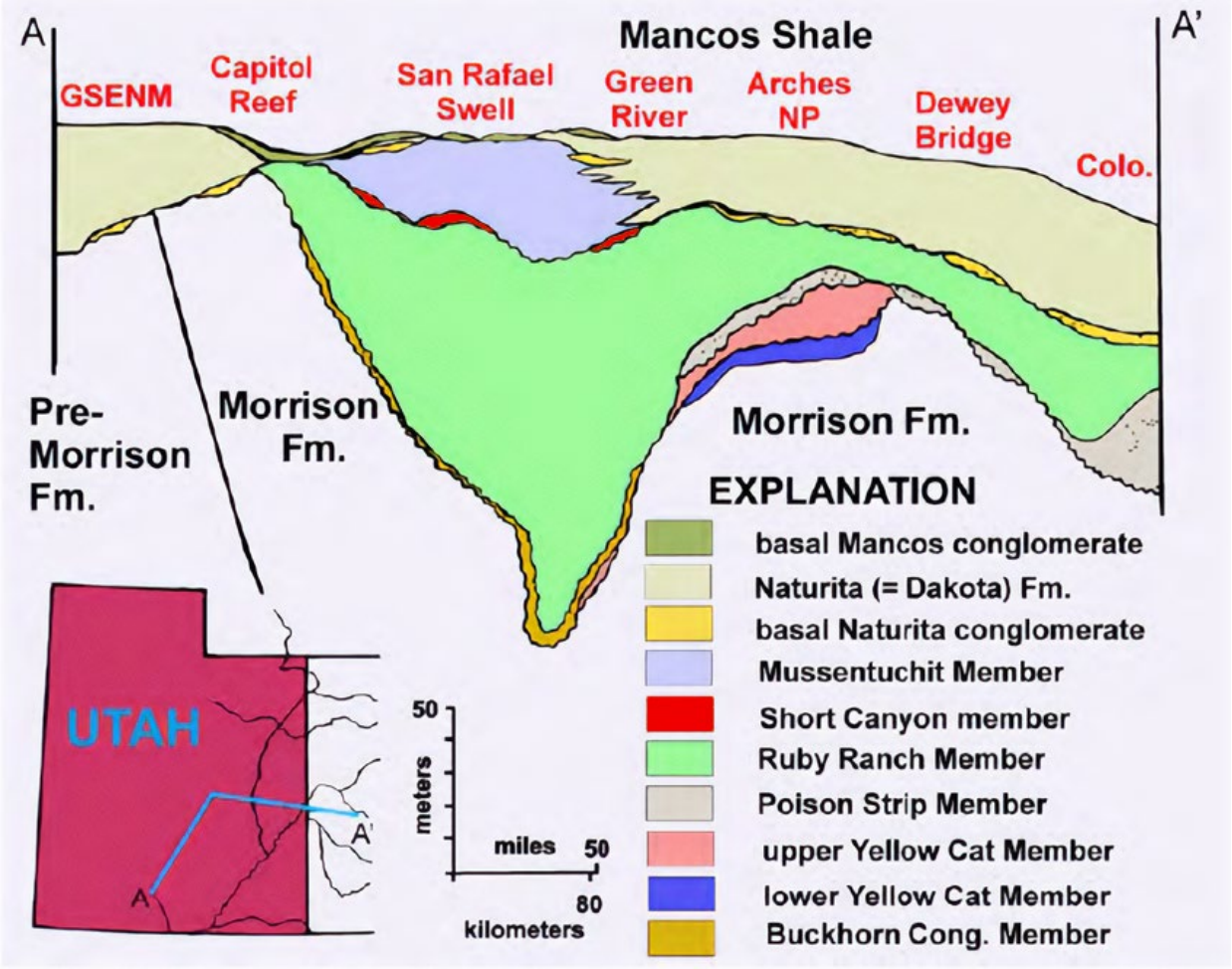

Figure 3: Simplified stratigraphic column of the Cedar Mountain Formation; Adapted from Figure 5 from Kirkland et al., (2016b). The Short Canyon member, from which these samples were taken, is in red between the Ruby Ranch and Mussentuchit Members.

Table 2

Water Availability Changes by Member of the Cedar Mountain Formation

MEMBER	ARID	HUMID	VERY HUMID
Mussentuchit			
Short Canyon			
Ruby Ranch			
Poison Strip			
Upper Yellow Cat			
Lower Yellow Cat			
Buckhorn			

Notes: The Short Canyon member did not have previous estimates of water availability, but the climate interpretations of the Short Canyon member from this thesis are added in pink. Climate estimates come from Kirkland et al. (2016b), Hatzell (2015), and Tucker et al., (2020).

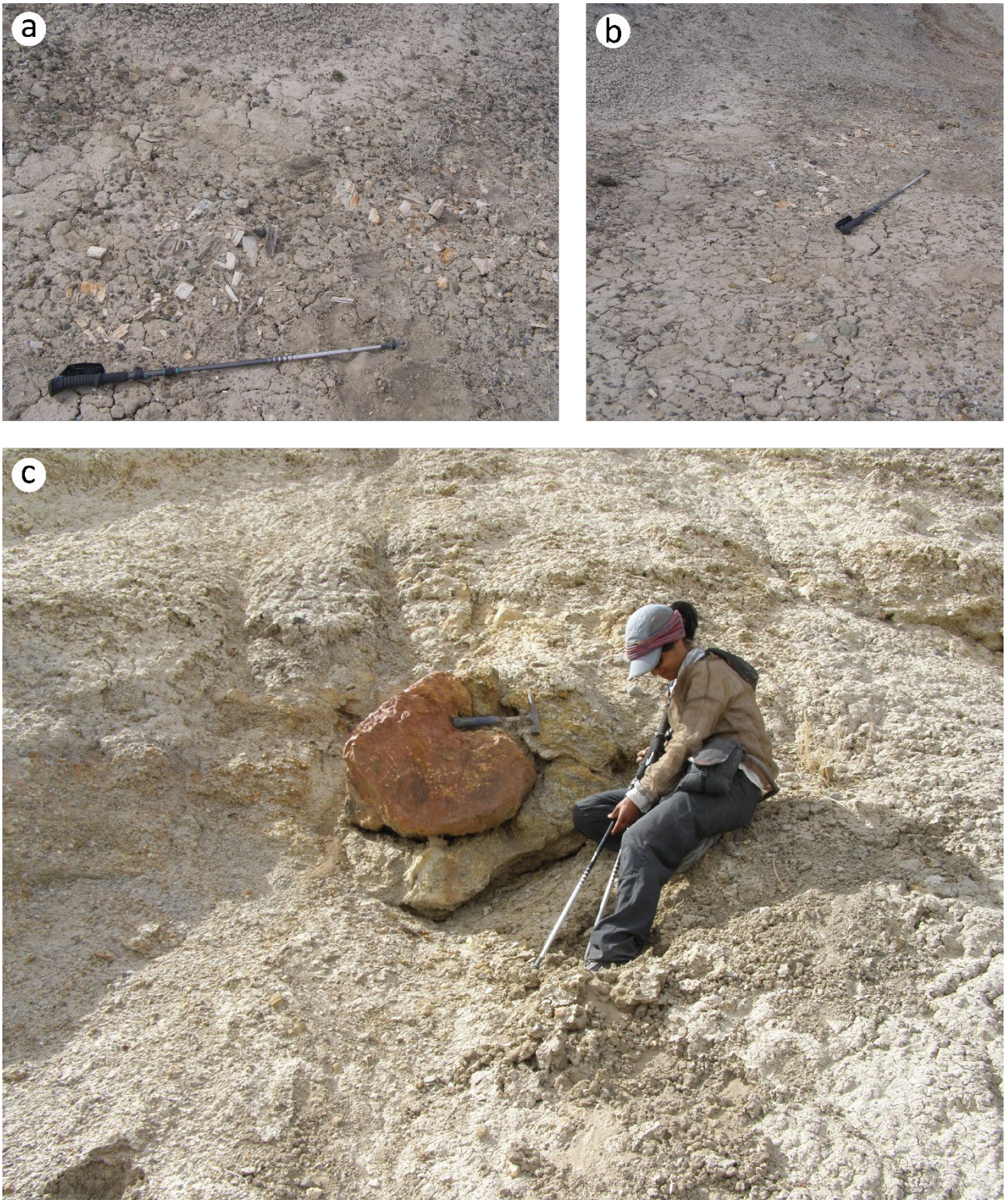

Figure 4: A&B) C2058 as it was discovered. Hiking poles for scale. **C)** *In situ* log in the Short Canyon Conglomerate about 2 meters north of C2058. Rock hammer and Dr. Celina Suarez for scale.

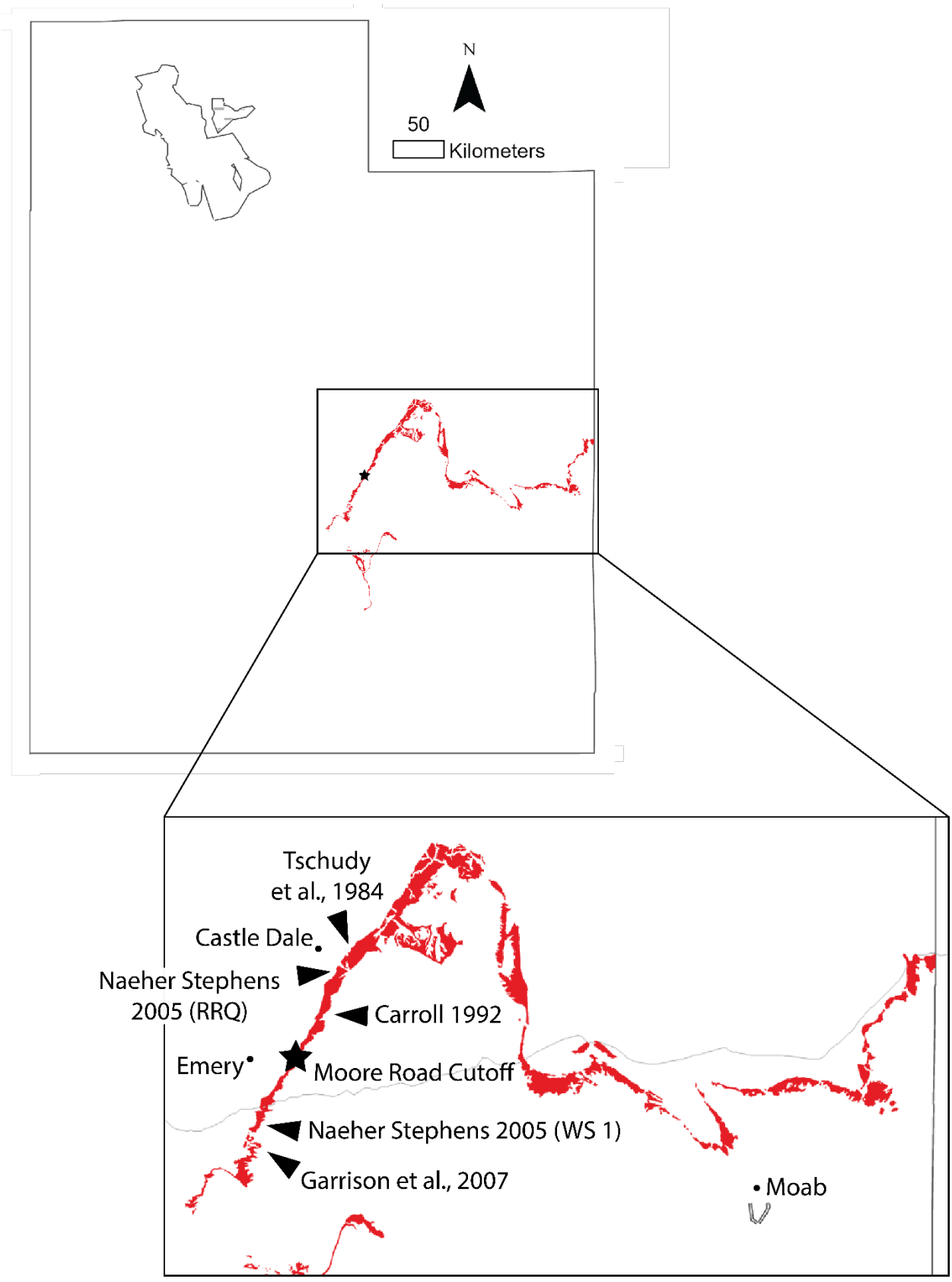
N
50
Kilometers
Tschudy
et al., 1984
Castle Dale
Naeher Stephens
2005 (RRQ)
Carroll 1992
Emery
Moore Road Cutoff
Naeher Stephens 2005 (WS 1)
Garrison et al., 2007
Moab

Figure 5: A map of the Cedar Mountain Formation outcrop in Utah. The star in the lower map is the Moore Road Cutoff Site, where the petrified wood fragment and palynology sediment sample studied in this thesis were collected. Also marked here are the sites from Tschudy et al. (1984), Carroll (1992), Garrison et al. (2007), and the two sites from Naeher Stephens (2005). The palynology results from these other studies, excluding Garrison et al. (2007), are available in Figure 9.

Table 3

A Summary of the Microscopic Characteristics of C2058.

SECTION	FEATURE	DESCRIPTION
Transverse	Growth rings	· Distinct and abrupt · False growth rings present
	Tracheids	· Rounded polygonal
	Axial Parenchyma	· Diffuse and abundant
Tangential	Rays	· Mostly uniseriate, up to triseriate · Opposite pairs, alternate when more · 1-(13)-65 cells tall; 56-(398)-1599um tall
Radial	Rays	· End walls smooth and thin
	Intertracheary Pitting	· Mostly uniseriate with biseriate pairs and zones · Usually opposite biseriate arrangement, occasionally alternate · Abietinean and mixed arrangement · Height:Width ratio: 0.96 · Crassulae present
	Crossfield Pitting	· 1-2 pits per crossfield, but up to 3 · Primarily taxodioid, frequently cupressoid, but can be glyptostroboid

Table 4

Abundances By Broad Plant Group of the Palynomorphs from the Moore Road Cutoff Site

	SLIDE 2		SLIDE 3		TOTAL	
	COUNT	**PERCENT**	**COUNT**	**PERCENT**	**COUNT**	**PERCENT**
Pteridophyte	169	87.6%	139	88.0%	308	87.8%
Angiosperm	10	5.2%	9	5.7%	19	5.4%
Gymnosperm	14	7.3%	10	6.3%	24	6.8%
Total	**193**	--	**158**	--	**351**	--

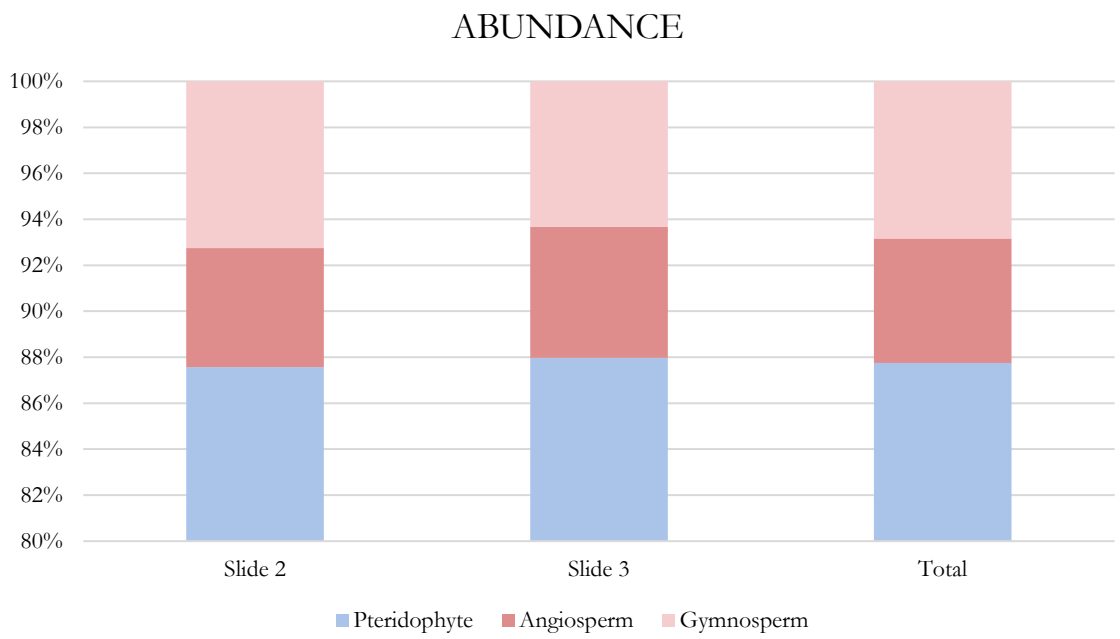

Figure 6: A stacked bar graph of the abundances of the major groups of terrestrial palynomorphs from Short Canyon member at the Moore Road Cutoff Site, Utah.

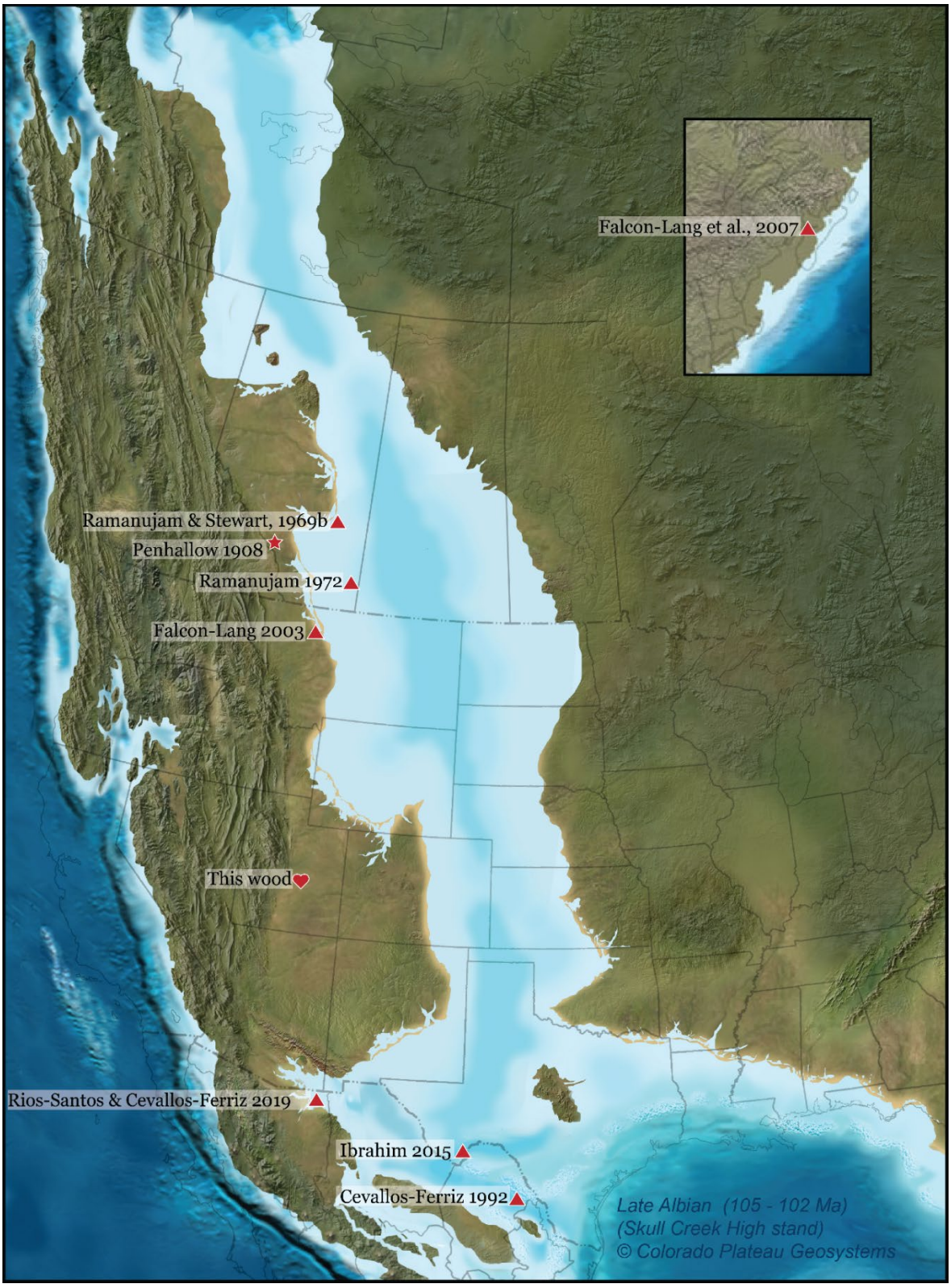

Figure 7: A map of Cretaceous *Taxodioxylon* in North America. The type specimen of *T. albertense* is indicated by the star, while this study is indicated by the heart.

Table 5

Other Findings of Taxodioxylon from the Cretaceous of North America

AUTHOR	TAXA	AGE
Rios-Santos and Cevallos-Ferriz 2019	*T. cabullensis*	Santonian to Late Maastrichtian
Penhallow 1908	*T. albertense*	Maastrichtian
Ramanujam and Stewart 1969b	*T. drumhellerense* *T. gypsaceum* *T. multiseriatum* *T. taxodii*	Maastrichtian
Cevallos-Ferriz 1992	*Taxodioxylon* sp.	Maastrichtian
Ramanujam 1972	*T. cryptomerioides* *T. multiseriatum*	Campanian
Falcon-Lang 2003	c.f. *Taxodioxylon* (resembles *T. cryptomerioides*)	Campanian
Ibrahim 2015	*Taxodioxylon* sp.	Campanian
Falcon-Lang et al., 2007	*Taxodioxylon* sp. (resembles *T. gypsaceum*)	Valanginian-Hauterivian

Notes: Most are from the Campanian to the Maastrichtian, but one dates to the Valanginian to the Hauterivian, which is early Cretaceous.

Table 6

Comparisons Between C2058 and Other Taxodioxylon Species from North America

		Reference	This study	Shikamura 1937, Kim 2005	Penhallow 1908	Ramanujam 1972		Cevallos-Ferriz 1992
		Taxa	C2058	*T. albertense*	*T. albertense*	*T. multiseriatum*	*T. cryptomerioides*	*Taxodioxylon sp.*
Transverse	Growth Rings	Present?	+	+	+	+	+	+
		Boundaries	ds	ds	ds	ds	ds	ds
		Transition	at	gl	at	gl	at	at
		Intraseasonal Rings	++	?	+-	-	-	+
	Tracheids	Shape	p, r	r	r, p	r	r	c
	Rays	Cells between Rays	1-(3.6)-8	1-(3.5)-8	2-8	1-3	--	1-6
Tangential	Rays	Height (cells)	1-(13)-65	1-(16)-61	1-54	2-70	1-20	2-40
		Uniseriate	++	++	++	++	++	++
		Biseriate	+	+-	+	+-	+-	+--
		Multiseriate	+-- (tri-)	+-- (tri-)	?	+-- (tetra-)	-	-
	Tracheids	Intertracheary pits	-	-+	++	-	-	+
Radial	Radial tracheid pits	Uniseriate	++	++	++	+-	++	++
		Biseriate	+-	+-	+-	++	+-	+-
		Triseriate	-	-	-	+-	-	-
		Arrangement	ab, mx	ab, mx	ab, mx	mx	mx	ab
		Biseriate arrangement	op, al +--	op	op	op	op	op
		Pit shape	c, ov	c, ov	c, ov	c	c	c
		Crassulae	+	+	?	+	+-	+
	Ray Cells	End walls	sm	sm	sm	sm	sm	sm
	Crossfield Pitting	Count	1-2, up to 3	1-2	1-2	1-4	1-4	1-2
		Type	tx ++, cu +, pd +-, gs +--	tx	cu	tx, cu +-	tx	cu (tx?)
All Sections	Axial Parenchyma	Present?	++	++	++	++	+	+
		Arrangement	df, zn +--	df, zn	df, zn	df	df	df
	Resin Canals	Axial	-	+-	-	-	-	-
		Traumatic	-	++	-	-	-	-
	Other							

Table 6 (cont.)

		Reference	This study	Falcon-Lang 2003	Falcon-Lang et al., 2007	Ibrahim 2015
		Taxa	C2058	*c.f. Taxodioxylon*	*Taxodioxylon sp.*	*Taxodioxylon sp.*
Transverse	Growth Rings	Present?	+	+	+-	+
		Boundaries	ds, ids	ds	ids, ds	ds
		Transition	at	gl	?	gl, at
		Intraseasonal Rings	++	+	-	+
	Tracheids	Shape	r, p	c, r	c, p	r
	Rays	Cells between Rays	1-3	1-9	--	--
Tangential	Rays	Height (cells)	1-30, up to 58	1-28	3-30	1-(18)-25
		Uniseriate	++	++	++	++
		Biseriate	+--	-	+-	+-
		Multiseriate	-	-	-	-
	Tracheids	Intertracheary pits	+-	-	?	-
Radial	Radial tracheid pits	Uniseriate	++	++	++	++
		Biseriate	+-	+-	+-	+-
		Triseriate	-	+-	-	-
		Arrangement	ar, mx	mx	ab	ab
		Biseriate arrangement	op, al +-	op, al +-	op	op
		Pit shape	c	c, r	c, p	c
		Crassulae	+	?	?	-
	Ray Cells	End walls	sm	sm	sm	sm
	Crossfield Pitting	Count	1-4	1-3, up to 4	1-2	1-9 (2-4)
		Type	cu, tx	tx	tx	cu ++, tx +--
All Sections	Axial Parenchyma	Present?	+	+	+-	++
		Arrangement	df	zn (?)	df	df
	Resin Canals	Axial	-	-	--	-
		Traumatic	-	-	--	-
	Other			weak spiral checking	common spiral checking	septate tracheids

Table 6 (cont.)

		Reference	This study	Ramanujam and Stewart 1969b			Rios-Santos and Cevallos-Ferriz 2019
		Taxa	C2058	*T. drumhellerense*	*T. gypsaceum*	*T. taxodii*	*T. cabullensis*
Transverse	Growth Rings	Present?	+	+	+	+	+
		Boundaries	ds	ds	ds	ds	ds
		Transition	gl	at	at	gl, at	gl, at
		Intraseasonal Rings	?	?	?	+	+
	Tracheids	Shape	r, p	r, p	r, p	r	r
	Rays	Cells between Rays	3-8	4-10	3-8	--	--
Tangential	Rays	Height (cells)	2-25	2-35	3-55	1-(18)-25	1-(18)-25
		Uniseriate	++	++	++	++	++
		Biseriate	+-	+-	+-	+-	+-
		Multiseriate	-	-	-	-	-
	Tracheids	Intertracheary pits	+-	+	+-	-	-
Radial	Radial tracheid pits	Uniseriate	++	++	++	++	++
		Biseriate	+-	+-	+-	+-	+-
		Triseriate	-	+--	+-	-	-
		Arrangement	mx	mx	ab, mx	ab	ab
		Biseriate arrangement	op, al +--	op	op	op	op
		Pit shape	c	c, ov	c	c	c
		Crassulae	+	++	++	-	-
	Ray Cells	End walls	sm	sm	sm	sm	sm
	Crossfield Pitting	Count	1-4, up to 6	2-8	2-4, up to 6	1-9 (2-4)	1-(2-4)-9
		Type	tx, gs	tx, cu	tx, cu	cu ++, tx +--	cu++, tx +--
All Sections	Axial Parenchyma	Present?	++	++	++	++	++
		Arrangement	df	zn	df, zn	df	df
	Resin Canals	Axial	-	-	-	-	-
		Traumatic	-	-	-	-	-
	Other			spiral checking		trabeculae	

Key to abbreviations: +, present; ++, abundant; +-, occasional; +--, rare; -, absent; ?, unknown; ds, distinct; ids, indistinct; at, abrupt; gl, gradual; c, circular; p, polygonal; r, rectangular; ov, oval; ab, abietinean; ar, araucarian; mx, mixed; op, opposite; al, alternate; sm, smooth; tx, taxodioid; cu, cupressoid; gs, glyptostroboid; pd, podocarpoid; df, diffuse; zn, zonate

Table 7

Locations and Ages of Other Findings of T. albertense

AUTHOR	LOCATION	CONTINENT	AGE
Velitzelos and Zouros 2006	Lesvos Petrified Forest Park at Bali Alonia	Europe	Miocene
Penhallow 1908	100 miles west of Gleichen, Alberta	North America	Maastrichtian (Srivastava 1968)
Kim et al., 2002	Gwanmaedo, South Korea	Asia	Campanian to Maastrichtian (Oh et al., 2011)
Meijer 2000	Rouscheweide quarry, Montzen, Belgium	Europe	middle to late Santonian
Shimakura 1937	Hirono, Fukushima Prefecture, Japan	Asia	Coniacian to Maastrichtian
	Futaba, Fukushima Prefecture, Japan	Asia	Coniacian to Maastrichtian
Shimakura 1940	Kawakami coal mine, Sakhalin Oblast, Russia	Asia	Coniacian to Maastrichtian
Nishida and Nishida, 1986	Bykov, Sakhalin Oblast, Russia	Asia	late Turonian-Santonian

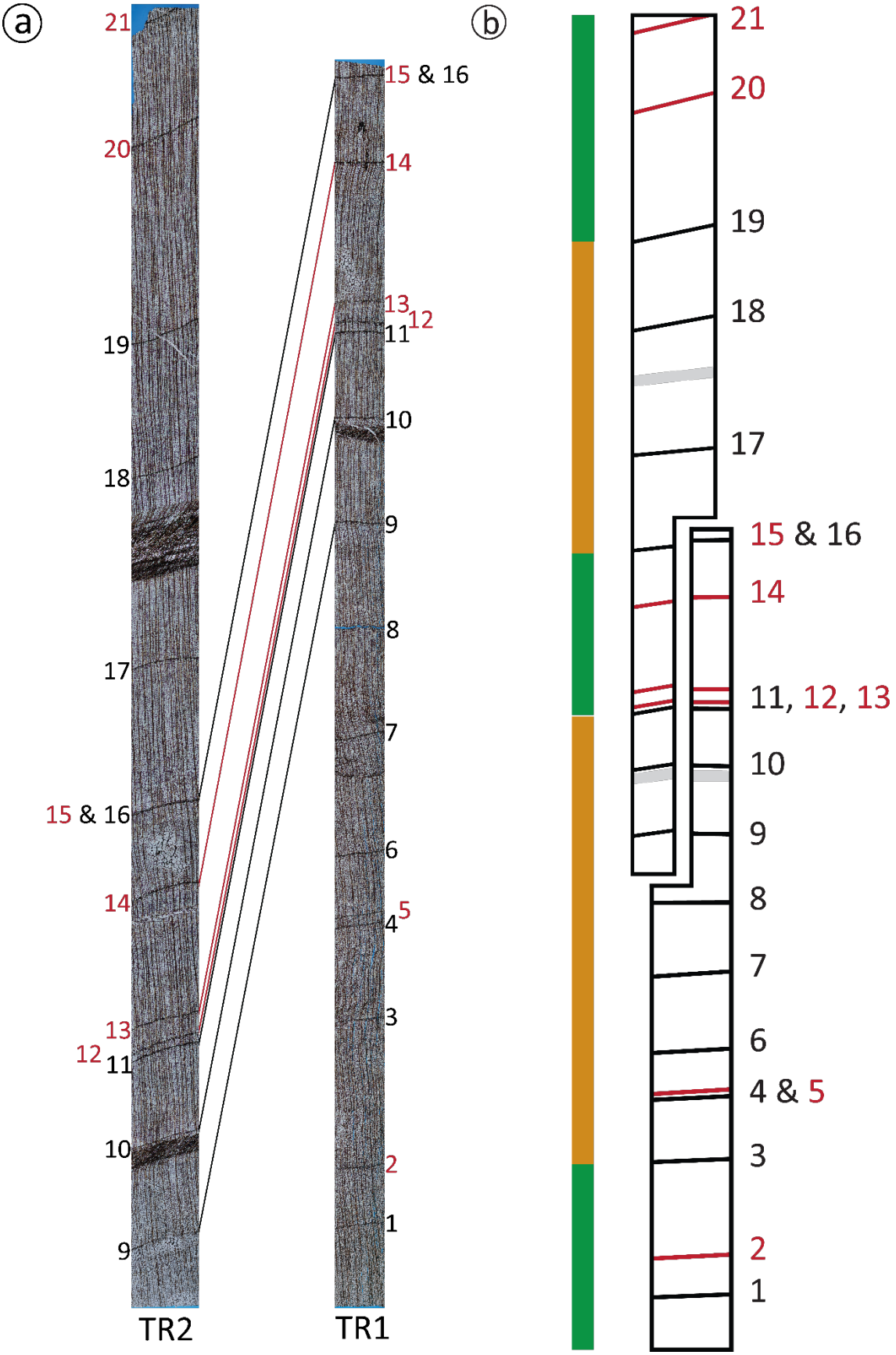
a
21
20
19
18
17
15 & 16
14
13
12
11
10
9
TR2
15 & 16
14
13
12
11
10
9
8
7
6
5
4
3
2
1
TR1
b
21
20
19
18
17
15 & 16
14
11, 12, 13
10
9
8
7
6
4 & 5
3
2
1

Figure 8: *Transverse section* Growth Ring Series showing the correlation of the rings from the two transverse slides. These were cut to have some overlap to extend the growth ring series, then stitched together in Photoshop. Seasonal growth rings are numbered in black, while intraseasonal growth rings are numbered in red. **A)** The stitched growth ring series with corresponding rings connected by lines. **B)** A simplified version of Figure 8a, with water regime indicated on the left. Orange indicates aridity while green indicates humidity.

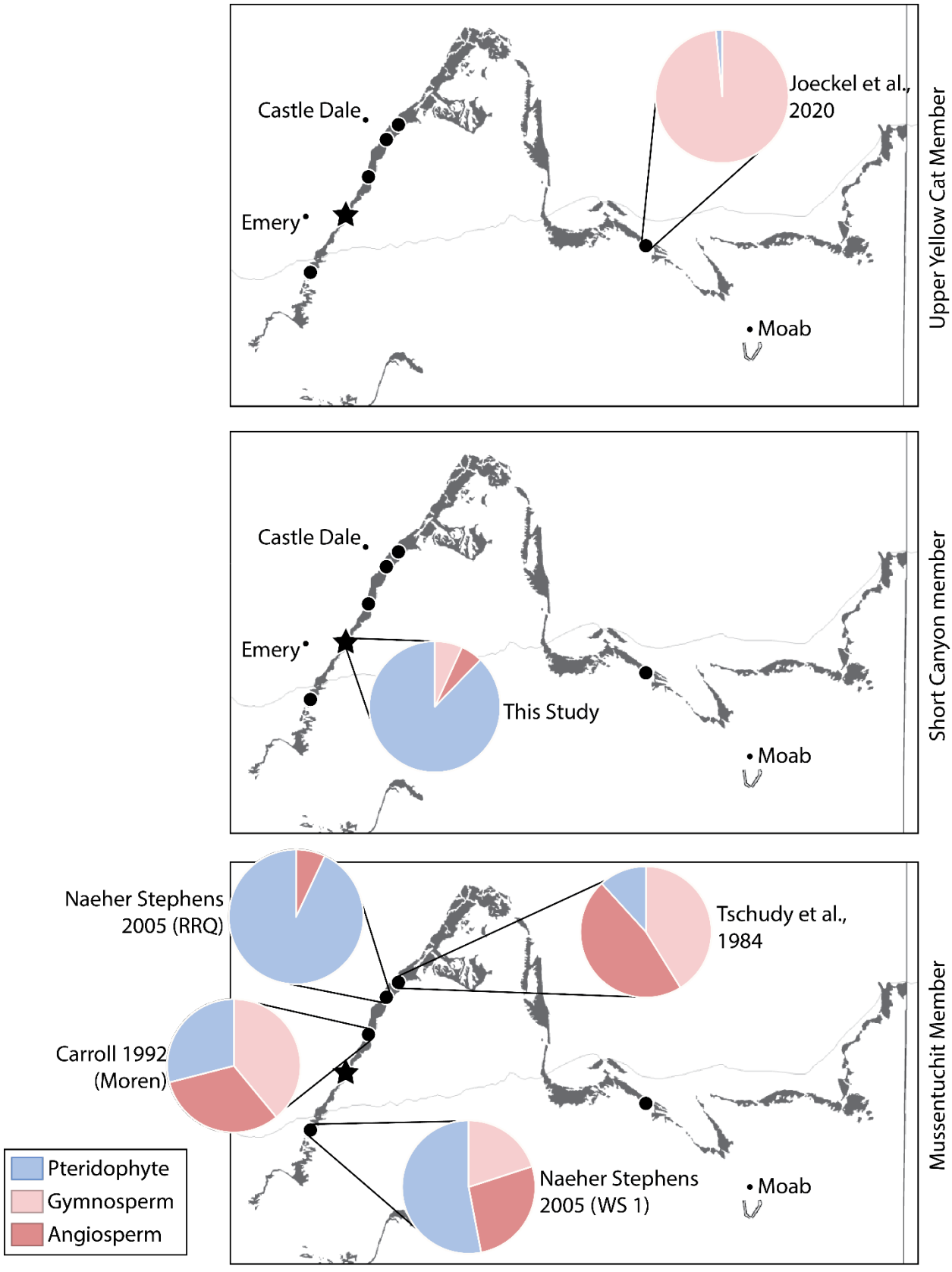
Castle Dale
Emery
Moab
Joeckel et al., 2020
Upper Yellow Cat Member
Castle Dale
Emery
This Study
Moab
Short Canyon member
Naeher Stephens 2005 (RRQ)
Tschudy et al., 1984
Carroll 1992 (Moren)
Naeher Stephens 2005 (WS 1)
Moab
Mussentuchit Member
Pteridophyte
Gymnosperm
Angiosperm

Figure 9: Maps of the Cedar Mountain Formation with palynology abundance results from various studies separated by member. The upper map represents the upper Yellow Cat Member, the middle the Short Canyon, and the bottom the Mussentuchit.

PLATES

Plate I.-Growth ring variability and tracheid shape in a tracheiodoxyl of *Taxodioxylon albertense* (Penhallow) Shimakura from the Short Canyon member of the Cedar Mountain Formation, Emery County, Utah. Specimen C2058, Natural History Museum, University of Kansas. Scale bar as indicated.

Figure 1) A seasonal growth ring (white arrow, ring 11 in the growth ring series) with two intraseasonal growth rings (red arrows, rings 12 and 13). In the seasonal growth ring, cell walls thicken in the latewood and the transition from latewood back into earlywood is abrupt. In the intraseasonal rings, cell walls do not thicken and the transition from latewood back into earlywood is nearly all gradual. The black arrow indicates axial parenchyma, which are smaller than tracheids, rectangular, and typically contain resin.

[Transverse section; TR1]

Figure 2) Another view of the bottom two growth rings (rings 11 and 12) in Figure 1. Here, the difference between the two types of growth ring is clearer.

[Transverse section; TR1]

Figure 3) Two growth rings that diverge and reconnect (rings 15 and 16 in Figure 8). The areas where the two rings converge are the deepest latewood seen in C2058, showing the shallowness of the growth rings.

[Transverse section; TR2]

Figure 4) The best-preserved tracheids in C2058. They are rounded squares or polygonal.

[Transverse section; TR2]

Figures 5 & 6) Resin leaking into tracheids from rays (5) and from intercellular spaces (6). This sample is highly resiniferous.

[Fig. 5: Transverse section; TR2]

[Fig. 6: Transverse section; TR1]

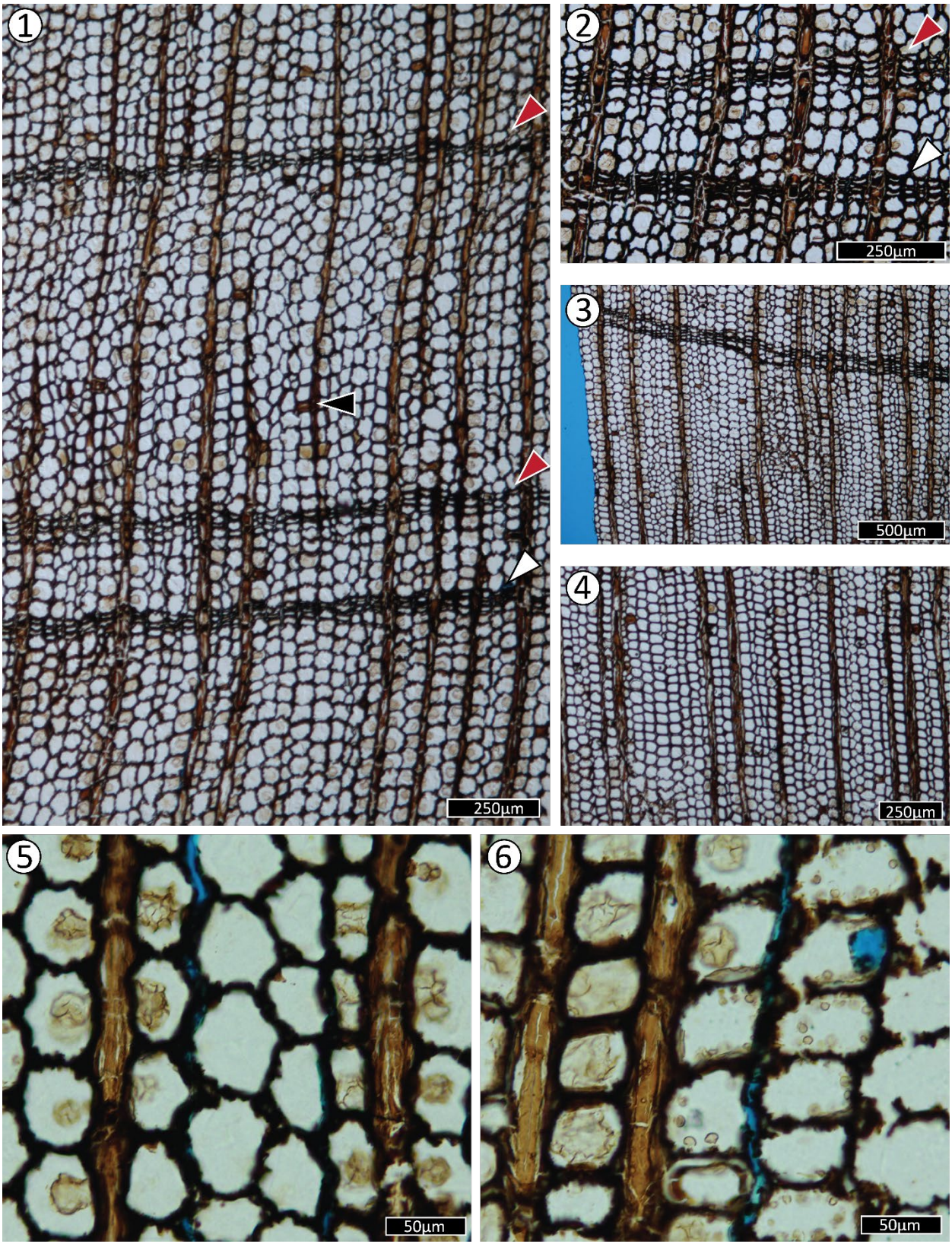
1
250µm
2
250µm
3
500µm
4
250µm
5
50µm
6
50µm

Plate II.-Tangential overview of *T. albertense*, showing the prevalence of axial parenchyma and the diversity of the width and height of rays.

Figure 1) In this view, three different ray widths are seen. The most common, uniseriate, is indicated by the black arrow. This specific ray is very tall; in this picture, 42 cells are shown. Localized biseriation is indicated by the red and blue arrows. The red arrow indicates a single opposite pair of ray parenchyma, while the blue indicates a larger area of biseriation. This type of arrangement is very common in *Taxodioxylon*. The white arrow indicates a triseriate ray with a very crowded arrangement.

[Tangential section; TR]

Figure 2) Axial parenchyma as it appears in tangential section, as indicated by the black arrow. Another triseriate ray can be seen just above the scale bar, as well as radial intertracheary pits.

[Tangential section; TR]

Figure 3) Two more strands of axial parenchyma with well-defined radial intertracheary pits.

[Tangential section; TR]

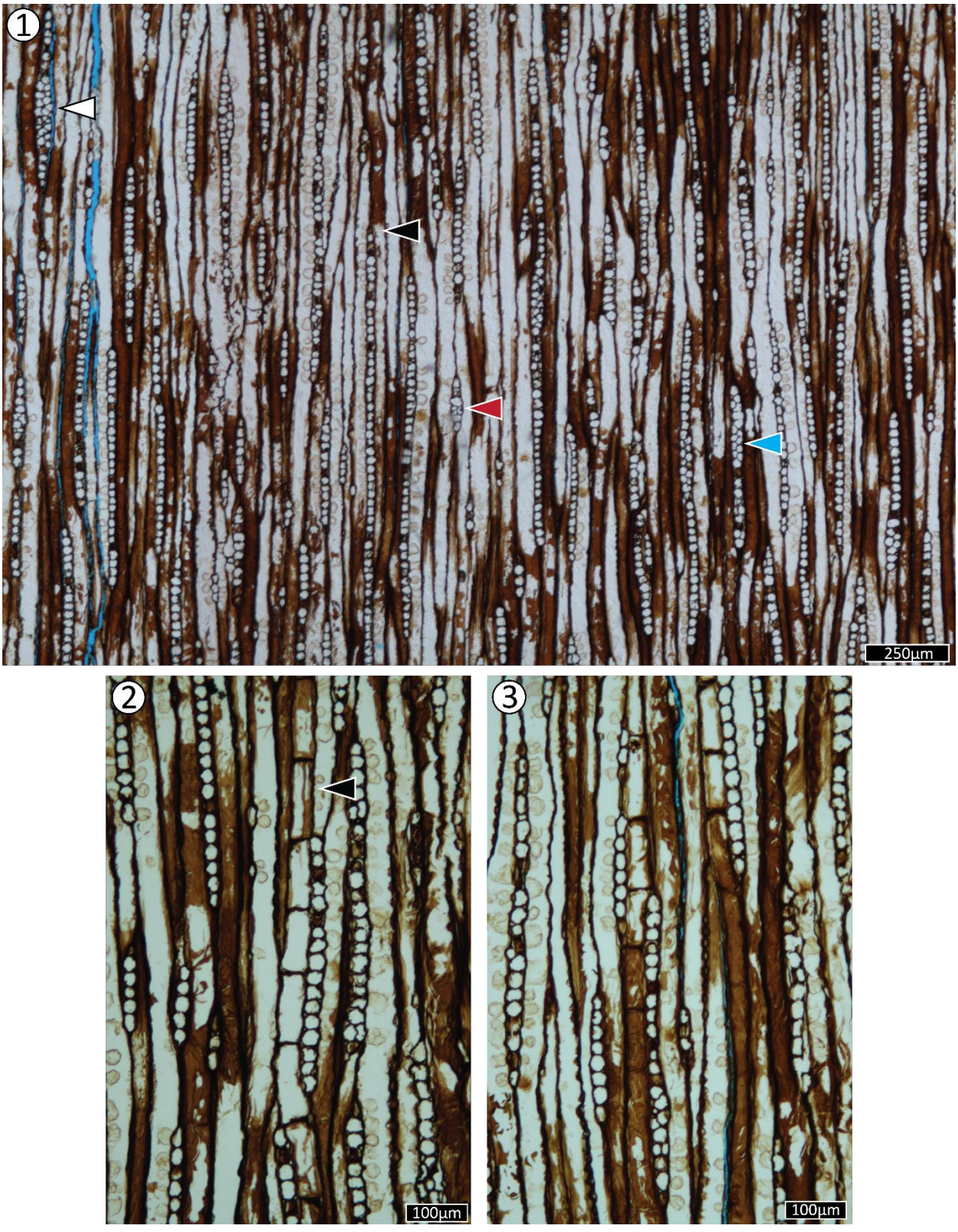
1
250µm
2
100µm
3
100µm

Plate III.-Variations in intertracheary pit arrangement and ray end walls.

Figure 1) Abietinean arrangement of uniseriate pits, with occasional opposite pairs of bordered pits present.

[Radial section; RD]

Figure 2) Abietinean to mixed arrangement of biseriate pit pairs, which are usually opposite but a few pairs with a subopposite to alternate arrangement are present. Crassulae can be seen in the lower portion of the figure.

[Radial section; RD]

Figure 3) Very distinct crassulae can be seen between these intertracheary bordered pits, which appear to have preserved tori.

[Radial section; RD]

Figure 4) Ray parenchyma end walls that are smooth and thin.

[Radial section; RD]

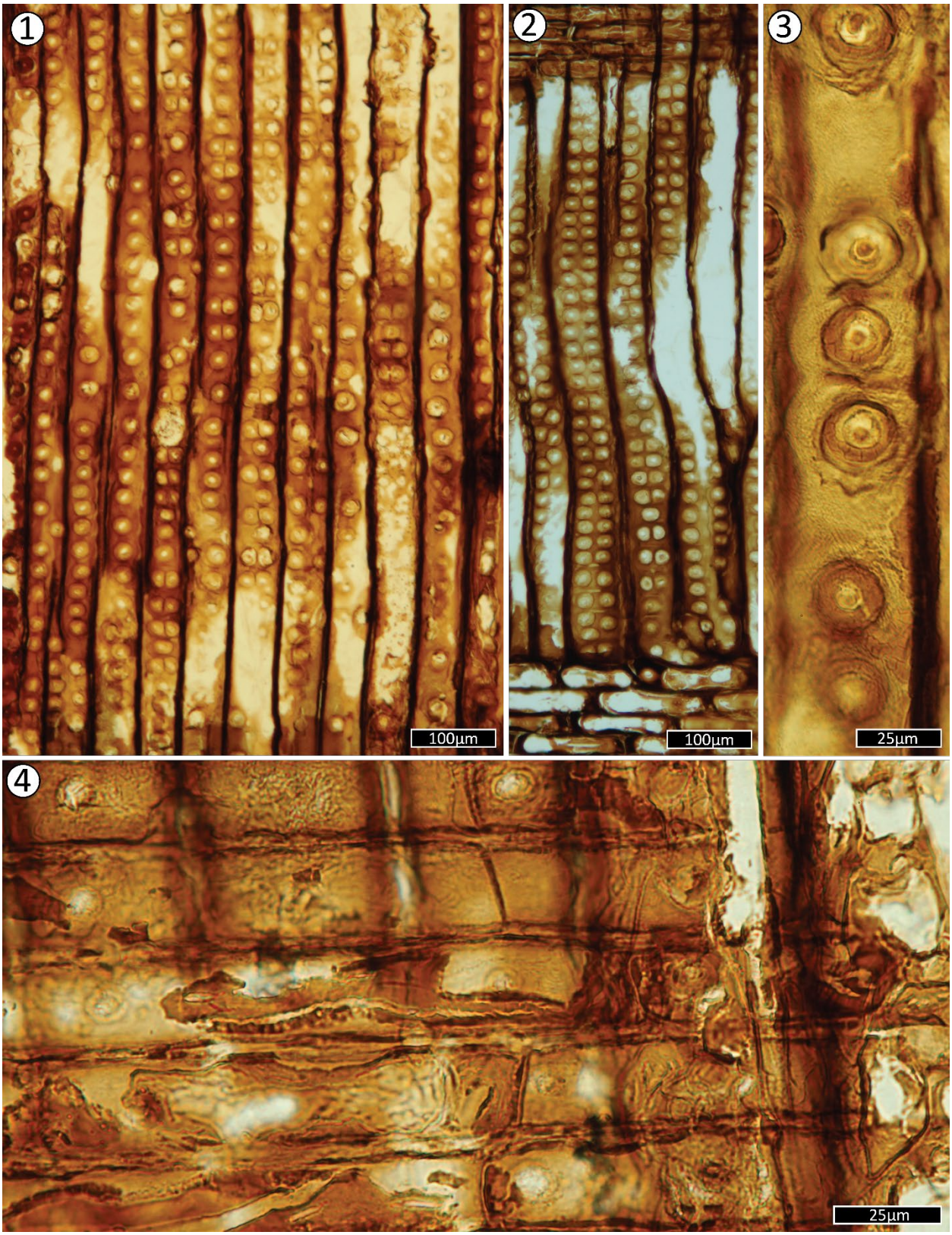
1
100µm
2
100µm
3
25µm
4
25µm

Plate IV.-The diversity of crossfields in C2058.

Figure 1) The most common arrangement of crossfield pitting in C2058: one (white arrow) or two (black arrow) taxodioid pits per crossfield; when multiple, are arranged horizontally.

[Radial section; RD]

Figure 2) Slightly more atypical crossfields, with variability in size, type (black arrow indicates more cupressoid pitting), and a more erratic arrangement.

[Radial section; RD]

Figure 3) 2-3 glyptostroboid crossfield pits in a two-row arrangement. Three crossfield pits per crossfield does not occur very frequently.

[Radial section; RD]

Figure 4) 1-2 podocarpoid crossfield pits with a regular horizontal arrangement.

[Radial section; RD]

Figure 5) 1 cupressoid pit per crossfield with erratic placements.

[Radial section; RD]

Figure 6) 1-2 diagonally arranged cupressoid pits.

[Radial section; RD]

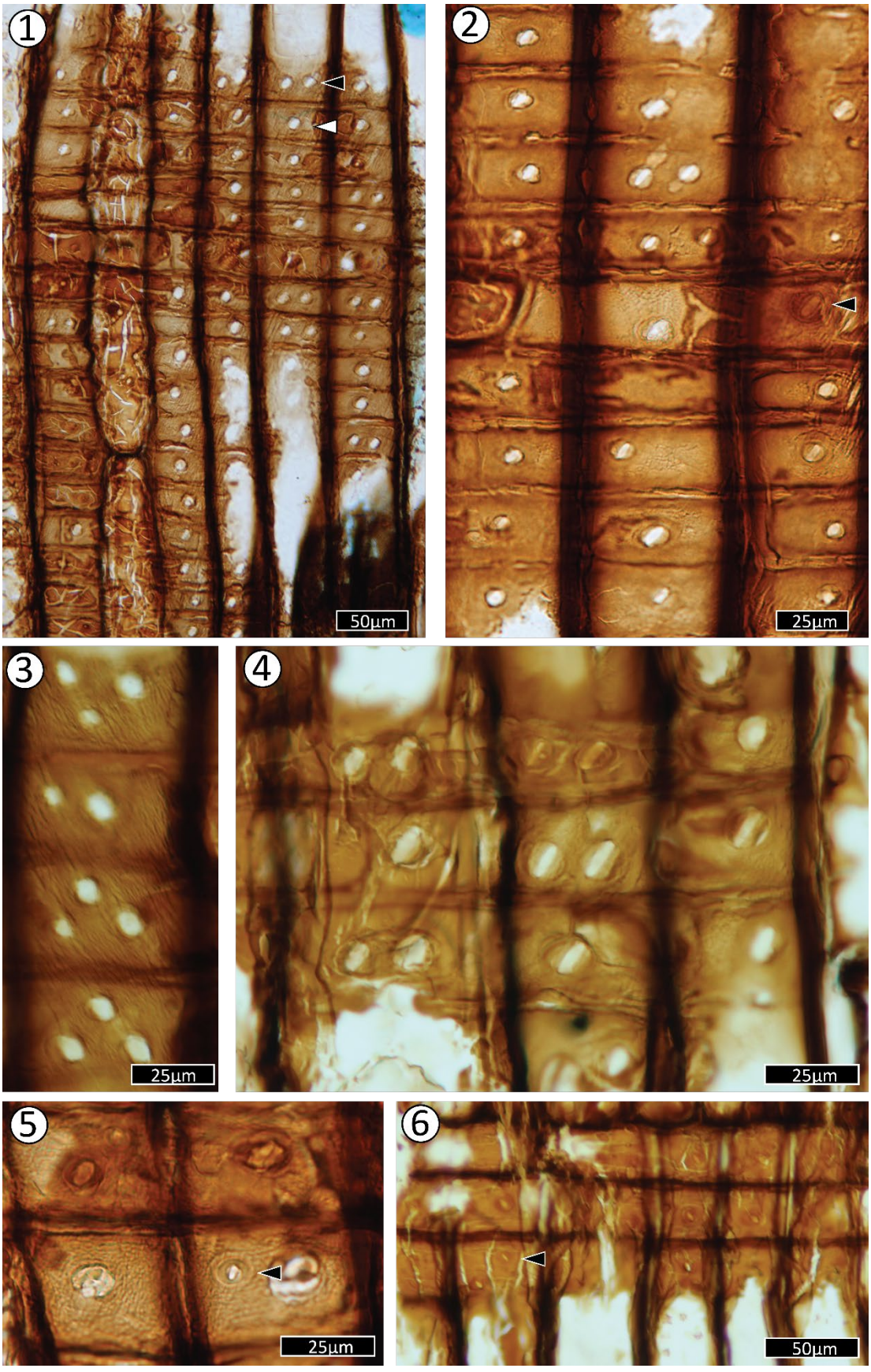
1
50µm
2
25µm
3
25µm
4
25µm
5
25µm
6
50µm

Plate V.-The insect boring. This is seen in the radial section of C2058 and is suspected to have been bored by a beetle or wasp, then colonized by an insect akin to a springtail, which left the frass.

Figure 1) A wide view of the insect boring. There are masses at 90 degrees and 225 degrees. On the left side, the resin has pulled away from the wood. There is no wound healing observed.

[Radial section; RD]

Figure 2) A close view of the masses in the boring, highlighting a long section of a fungal hypha. Fungal hyphae make up the bulk of the masses in the boring.

[Radial section; RD]

Figure 3) A close view of the only identified wood cells in the boring. Insect borings are frequently filled with wood cell frass, and this boring is unusual in that it only shows three cells.

[Radial section; RD]

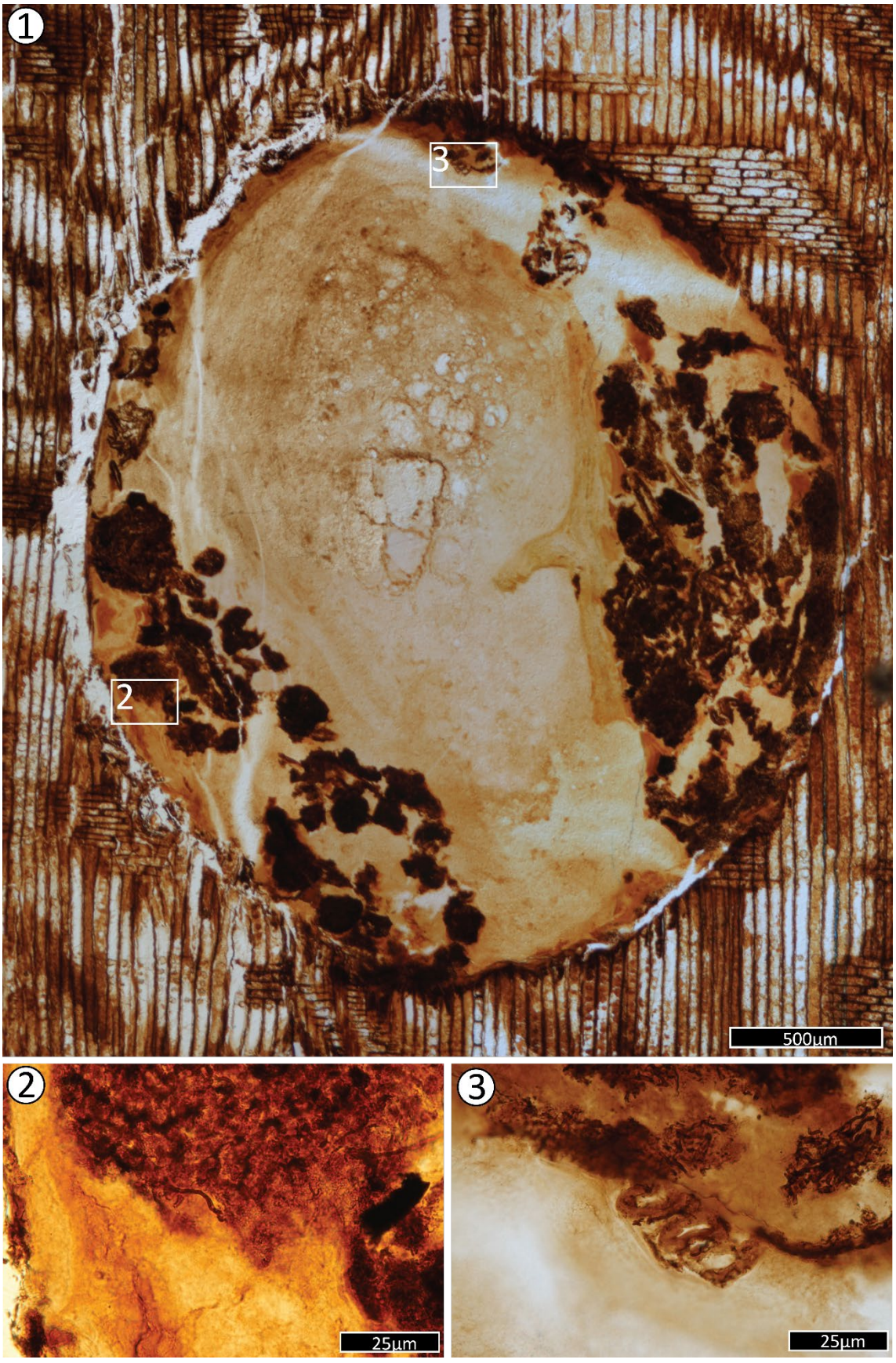
1
3
2
500µm
2
25µm
3
25µm

Plate VI.-Fungal hyphae in the body of the wood.

Figure 1) Fungal hypha with a rounded tip growing through the ray parenchyma.

[Radial section; RD]

Figure 2) Fungal hypha growing through successive tracheids in a poorly preserved section of the wood.

[Radial section; RD]

Figure 3) A network of fungal hyphae from very close to the insect boring.

[Radial section; RD]

Figure 4) A segmented fungal hypha growing along a tracheid.

[Radial section; RD]

Figure 5) A branching fungal hypha.

[Radial section; RD]

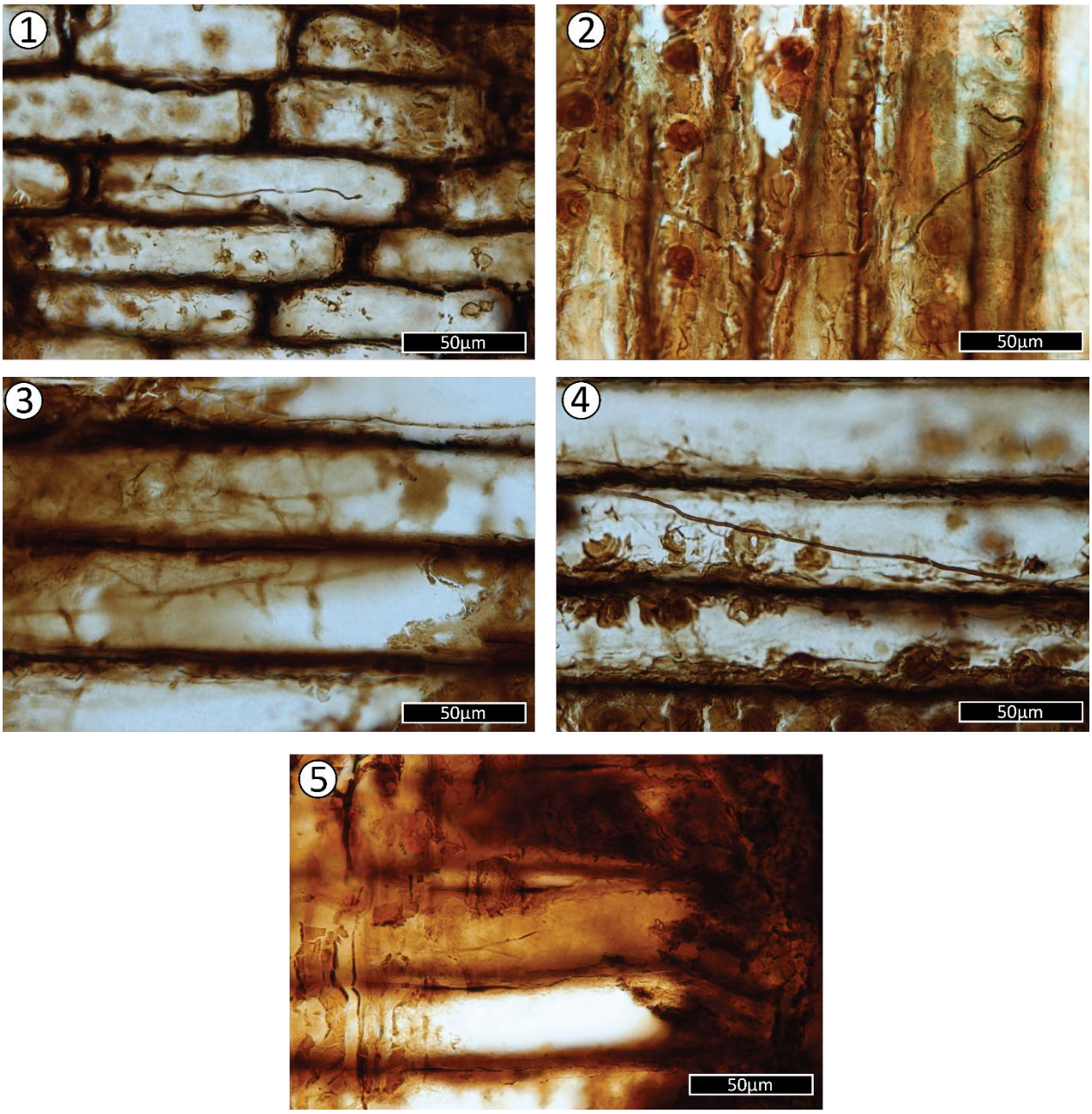
1
50µm
2
50µm
3
50µm
4
50µm
5
50µm

Plate VII.- Angiosperm features seen in wood fragments from the palynology slides. These samples came from the upper portion of the Short Canyon member.

Figure 1) Fibers with occasional minutely bordered pits.

Figure 2) Septate fibers with minutely bordered pits.

Figure 3) Fiber with half bordered pits.

Figure 4) Fiber with bordered pits. These are much smaller than the bordered pits in Plate VIII.

Figure 5) Potential nodular end wall of a parenchymatous cell.

Figure 6) Fiber cells (septate or intersection with ray parenchyma) with warty layers and resin globules. The minutely bordered pit indicates that these are fiber cells, and therefore this fragment originated in an angiosperm.

Figure 7) A long section of scalariform intervessel pitting. The number of bars (>40) indicates that this is more likely to be intervessel pitting rather than a scalariform perforation plate.

Figure 8) A wide section of scalariform intervessel pitting, showing at least 6 and up to 10 contiguous vessels.

Figure 9) Alternate intervessel pitting with oval apertures. The shape of the intervessel pits cannot be seen.

Figure 10) Subopposite to alternate intervessel pitting.

Figure 11) Scalariform to opposite intervessel pitting with pit borders visible.

Figure 12) Circular alternate intervessel pitting.

Figure 13) Polygonal alternate intervessel pitting with potentially vestured slit-shaped pit apertures.

Figure 14) Potential regularly reticulate perforation plate, but more likely to be alternate intervessel pitting.

Figure 15) Scalariform to opposite intervessel pitting. This could potentially also be a scalariform to reticulate perforation plate.

Figure 16) Similar to Figure 12, scalariform to opposite intervessel pitting.

Figure 17) Possible helical thickening, but could also be a regularly reticulate perforation plate, similar to Figure 9 below it.

Figure 18) Regularly reticulate to scalariform perforation plate. This form doesn't occur in intervessel pitting.

Figure 19) Potential vessel-ray pitting with reduced borders and vertical palisade arrangement.

Figure 20) Potential vessel-ray pitting with reduced borders and vertical palisade arrangement.

Figure 21) Potential vessel-ray pitting with reduced borders and vertical palisade arrangement.

Figure 22) A reticulate to foraminate perforation plate.

Figure 23) A reticulate perforation plate.

Figure 24) A foraminate perforation plate.


1
2
3
4
5
6
7
8
9
10
11
12
13
14
15
16
17
18
19
20
21
22
23
24
25µm

Plate VIII-Ambiguous and Gymnosperm features seen in wood fragments from the palynology slides. These samples came from the upper portion of the Short Canyon member.

Figure 1) Helical thickening across several cells. This could be either a gymnosperm or an angiosperm feature.

Figure 2) Pits that resemble crossfield pitting in gymnosperms, but could also represent gymnosperm bordered pits with crassulae.

Figure 3) Pits resembling cupressoid crossfield pits but could also represent bordered pits with crassulae.

Figure 4) A bordered pit that is typical for what is found in the wood fragments: round with a round aperture and generally distant from neighboring bordered pits.

Figure 5) Pits that are an intermediate between Figures 7 and 8. Here, the bars that resemble crossfields or crassulae are absent.

Figure 6) A pair of circular bordered pits with large circular apertures

Figure 7) A pair of bordered pits with narrow borders and elliptical apertures

Figure 8) Pits that most likely represent cupressoid crossfield pits, but may also represent bordered pits with crassulae.

Figure 9) Bordered pits with potential torus extensions.

Figure 10) Bordered pits with radiating torus extensions.

Figure 11) A very large oval bordered pit with oval aperture, fairly closely spaced in regard to the pit next to it, but not touching.

Figure 12) A series of small oval bordered pits with relatively large circular apertures.

Figure 13) A large oval bordered pit with an oval aperture.

Figure 14) A pair of bordered pits with visible tori.

Figure 15) Three bordered pits with visible tori.

Figure 16) Two pairs of biseriate bordered pits, one pair oppositely arranged and the other subopposite.

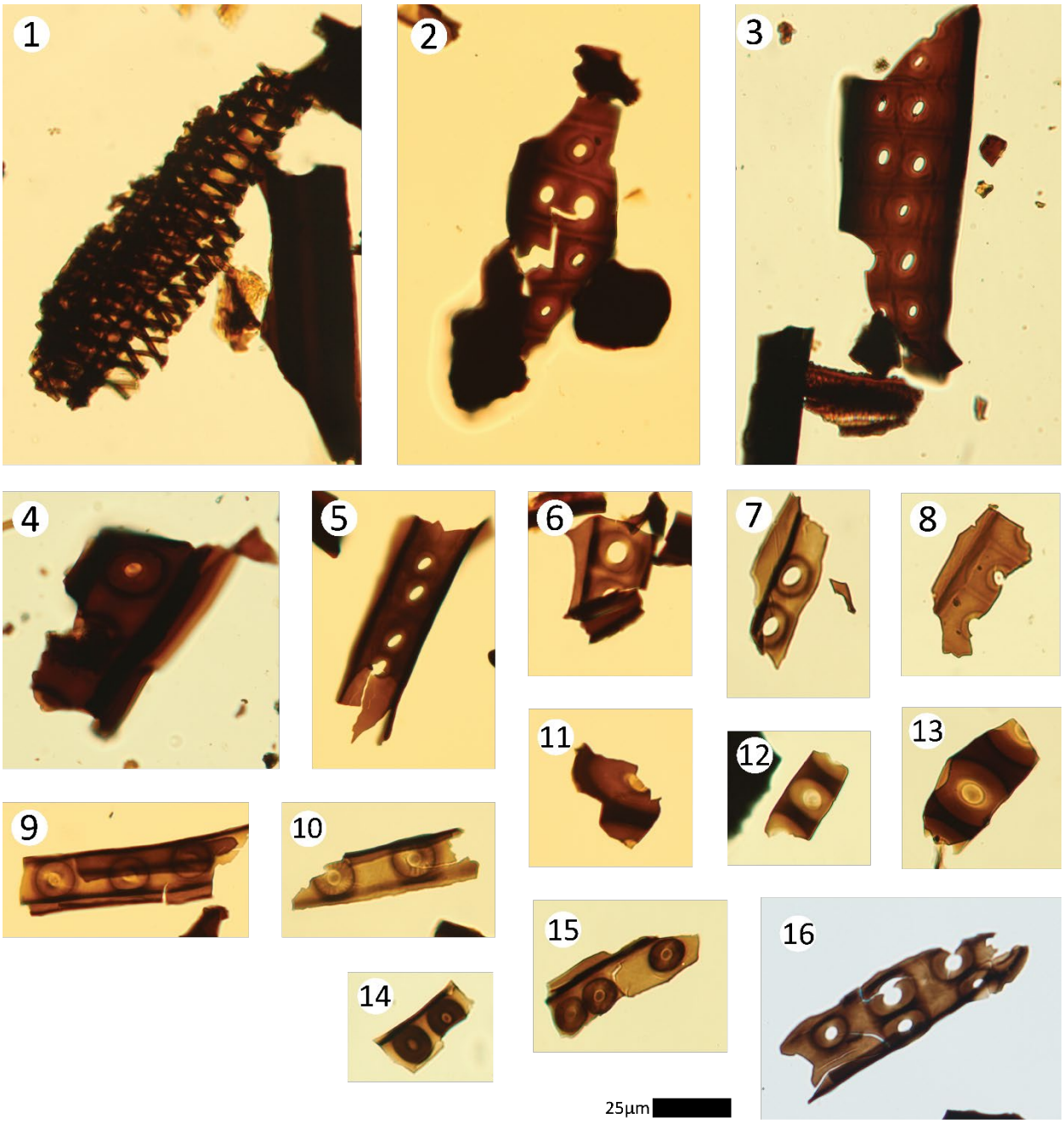
1
2
3
4
5
6
7
8
11
12
13
9
10
15
16
14
25µm

WORKS CITED

Akkemik, Ü., 2019, New fossil wood descriptions from the Pliocene of central Anatolia and the presence of *Taxodioxylon* in Turkey from the Oligocene to Pliocene: Turkish Journal of Earth Sciences, v. 28, no. 3, p. 398–409, https://doi.org/10.3906/yer-1805-24.

Akre, R.D. and Hansen, L. D., 1990, Management of carpenter ants, *in* Vander Meer, R.K., Jaffe, K., and Cedeno, A., eds., Applied Myrmecology: A World Perspective: Boulder, Colorado, Westview Press, p. 693–700.

Arens, N.C., and Gleason, J.P., 2016, Insect folivory in an angiosperm-dominated flora from the mid-Cretaceous of Utah, U.S.A.: PALAIOS, v. 31, no. 3, p. 71–80, https://doi.org/10.2110/palo.2015.032.

Avrahami, H.M., Gates, T.A., Heckert, A.B., Makovicky, P.J., and Zanno, L.E., 2018, A new microvertebrate assemblage from the Mussentuchit Member, Cedar Mountain Formation: Insights into the paleobiodiversity and paleobiogeography of early Late Cretaceous ecosystems in western North America: PeerJ, v. 6, e5883. https://doi.org/10.7717/peerj.5883.

Bakker, R.T., 1986, The dinosaur heresies: new theories unlocking the mystery of the dinosaurs and their extinction. New York, Morrow.

Bao, T., Wang, B., Li, J., and Dilcher, D. ,2019, Pollination of Cretaceous flowers: Proceedings of the National Academy of Sciences, v. 116, no. 49, p. 24707–24711, https://doi.org/10.1073/pnas.1916186116.

Barton, K.E., Howell, D.G., and Vigil, J.F., 2003, The North American Tapestry of Time and Terrain: United States Geological Survey, 1:8,000,000 scale

Benton, M.J., Wilf, P., and Sauquet, H, 2022, The Angiosperm Terrestrial Revolution and the origins of modern biodiversity: New Phytologist, v. 233, no. 5, p. 2017–2035, https://doi.org/10.1111/nph.17822.

Berendse, F., and Scheffer, M., 2009, The angiosperm radiation revisited, an ecological explanation for Darwin's 'abominable mystery': Ecology Letters, v. 12, no. 9, p. 865–872, https://doi.org/10.1111/j.1461-0248.2009.01342.x.

Bilbey, S.A., 1998, Cleveland-Lloyd Dinosaur Quarry - age, stratigraphy and depositional environments, *in* Carpenter, K., Chure, D., and Kirkland, J.I., eds., The Morrison Formation: An Interdisciplinary Study: Modern Geology, v. 22: Taylor and Francis Group, p. 87–120.

Boura, A., Bamford, M., and Philippe, M., 2021, Promoting a standardized description of fossil tracheidoxyls: Review of Palaeobotany and Palynology, v. 295, 104525, https://doi.org/10.1016/j.revpalbo.2021.104525.

Brikiatis, L., 2016, Late Mesozoic North Atlantic land bridges: Earth-Science Reviews, v. 159, p. 47–57, https://doi.org/10.1016/j.earscirev.2016.05.002.

Britt, B.B., Eberth, D.A., Scheetz, R.D., Greenhalgh, B.W., and Stadtman, K.L., 2009, Taphonomy of debris-flow hosted dinosaur bonebeds at Dalton Wells, Utah (Lower Cretaceous, Cedar Mountain Formation, USA): Palaeogeography, Palaeoclimatology, Palaeoecology, v. 280, p. 1–22, https://doi.org/10.1016/j.palaeo.2009.06.004.

Buschiazzo, E., Ritland, C., Bohlmann, J., and Ritland, K., 2012, Slow but not low: Genomic comparisons reveal slower evolutionary rate and higher dN/dS in conifers compared to angiosperms: BMC Evolutionary Biology, v. 12, no. 1, 8, https://doi.org/10.1186/1471-2148-12-8.

Camarero, J.J., Collado, E., Martínez-de-Aragón, J., de-Miguel, S., Büntgen, U., Martinez-Peña, F., Martín-Pinto, P., Ohenoja, E., Romppanen, T., Salo, K., Oria-de-Rueda, J.A., and Bonet, J.A., 2021, Associations between climate and earlywood and latewood width in boreal and Mediterranean Scots pine forests: Trees, v. 35, no. 1, p. 155–169, https://doi.org/10.1007/s00468-020-02028-0.

Carpenter, K., and Ishida, Y., 2010, Early and middle Cretaceous iguanodonts in time and space: Journal of Iberian Geology, v. 36, no. 2, p. 145–164, https://doi.org/10.5209/rev_JIGE.2010.v36.n2.3.

Carroll, A.L., Sillett, S.C., and Kramer, R.D., 2014, Millennium-scale crossdating and inter-annual climate sensitivities of standing California redwoods: PLoS ONE, v. 9, no. 7, e102545, https://doi.org/10.1371/journal.pone.0102545.

Carroll, R.E., 1992, Biostratigraphy and paleoecology of mid-Cretaceous sedimentary rocks, eastern Utah and western Colorado: a palynological interpretation [Ph.D. dissertation]: Michigan State University, 471 p.

Castaño-Meneses, G., Palacios-Vargas, J.G., Delabie, J.H.C., Zeppelini, D., and Mariano, C.S.F., 2017, Springtails (Collembola) associated with nests of fungus-growing ants (Formicidae: Myrmicinae: Attini) in southern Bahia, Brazil: Florida Entomologist, v. 100, no. 4, p. 740–742, https://doi.org/10.1653/024.100.0421.

Chaboureau, A.-C., Sepulchre, P., Donnadieu, Y., and Franc, A., 2014, Tectonic-driven climate change and the diversification of angiosperms: Proceedings of the National Academy of Sciences, v. 111, no. 39, p. 14066–14070, https://doi.org/10.1073/pnas.1324002111.

chasingthewhiteroom, October 28 2021, *Some massive 'In Situ' Petrified Wood specimens from the Cedar Mountain formation!* [Online forum post]. Reddit. https://www.reddit.com/r/rockhounds/comments/qhnmc8/some_massive_in_situ_petrified_wood_specimens/?utm_source=share&utm_medium=web2x&context=3

Christenhusz, M.J.M., and Byng, J.W., 2016, The number of known plants species in the world and its annual increase: Phytotaxa, v. 261, no. 3, 201, https://doi.org/10.11646/phytotaxa.261.3.1.

Copenheaver, C.A., Matiuk, J.D., Nolan, L.J., Franke, M.E., Block, P.R., Reed, W.P., Kidd, K.R., and Martini, G., 2017, False ring formation in bald cypress (*Taxodium distichum*): Wetlands, v. 37, p. 1037–1044, https://doi.org/10.1007/s13157-017-0938-9.

Crane, P.R. and Lidgard, S., 1988, Angiosperm diversification and paleolatitudinal gradients in Cretaceous floristic diversity: Science, v. 246, p. 675-678, DOI:10.1126/science.246.4930.675.

Creber, G.T., and Chaloner, W.G., 1984, Influence of environmental factors on the wood structure of living and fossil trees: The Botanical Review, v. 50, no. 4, p. 357–448, https://doi.org/10.1007/BF02862630.

Cross, A.T., Maxfield, E.B., Cotter, E., and Cross, C.C., 1975, Field guide and road log to the western Book Cliffs, Castle Valley and parts of the Wasatch Plateau. Brigham Young University Geol. Stud., v. 22, no. 2, p. 1-132.

Currie, B.S., 1998, Upper Jurassic-Lower Cretaceous Morrison and Cedar Mountain Formations, NE Utah-NW Colorado: Relationships between nonmarine deposition and early Cordilleran foreland-basin development: SEPM Journal of Sedimentary Research, v. 68, https://doi.org/10.1306/D426882E-2B26-11D7-8648000102C1865D.

Dayvault, R.D., and Hatch, H.S., 2005, Cycads: From the Upper Jurassic and Lower Cretaceous rocks of southeastern Utah: Rocks & Minerals, v. 80, no. 6, p. 412–432, https://doi.org/10.3200/RMIN.80.6.412-432.

Dayvault, R.D., and Hatch, H.S., 2007, Conifer cones from the Jurassic and Cretaceous rocks of eastern Utah: Rocks & Minerals, v. 82, no. 5, p. 382–397, https://doi.org/10.3200/RMIN.82.5.382-397.

Deng, W., De Franceschi, D., Xu, X., Del Rio, C., Low, S.L., Zhou, Z., Spicer, R.A., Ren, L., Yang, R., Tian, Y., Wu, M., Yang, J., Liang, S., Wappler, T., and Su, T., 2022, Plant–insect and –fungal interactions in *Taxodium*-like wood fossils from the Oligocene of southwestern China: Review of Palaeobotany and Palynology, v. 302, 104669, https://doi.org/10.1016/j.revpalbo.2022.104669.

Détienne, P., 1989, Appearance and periodicity of growth rings in some tropical woods: IAWA Journal, v. 10, no. 2, p. 123-132, https://doi.org/10.1163/22941932-90000480.

Dodd, R.S., and DeSilva, R., 2016, Long-term demographic decline and late glacial divergence in a Californian paleoendemic: *Sequoiadendron giganteum* (giant sequoia). Ecology Evolution, vol. 6, no. 10, p. 3342-55. doi: 10.1002/ece3.2122. PMID: 27252835; PMCID: PMC4870217.

Doelling, H.H., and Kuehne, P.A., 2013a, Geologic map of the Short Canyon quadrangle, Emery County, Utah: Utah Geological Survey Map 255DM, 31 p., 2 plates, scale 1:24,000, https://doi.org/10.34191/M-255dm.

Edmondson, J.R., 2010, The meteorological significance of false rings in eastern redcedar *(Juniperus virginiana L.*) from the southern Great Plains, U.S.A. Tree-Ring Res., vol. 66, no. 1, p. 19–33. https://doi.org/10.3959/2008-13.1

Elliot, W.S., Suttner, L.J., and Pratt, L.M., 2007, Tectonically induced climate and its control on the distribution of depositional systems in a continental foreland basin, Cloverly and Lakota formations (Lower Cretaceous) of Wyoming, U.S.A.: Sedimentary Geology, v. 202, p. 730-753, doi:10.1016/j.sedgeo.2007.09.001.

Esteban, L.G., de Palacios, P., Heinz, I., Gasson, P., García-Iruela, A., and García-Fernández, F., 2023, Softwood Anatomy: A Review: Forests, v. 14, no. 2, 323, https://doi.org/10.3390/f14020323.

Falcon-Lang, H.J., 2003, Growth interruptions in silicified conifer woods from the Upper Cretaceous Two Medicine Formation, Montana, USA: Implications for palaeoclimate and dinosaur palaeoecology: Palaeogeography, Palaeoclimatology, Palaeoecology, v. 199, no. 3–4, p. 299–314, https://doi.org/10.1016/S0031-0182(03)00539-X.

Falcon-Lang, H.J., and Cantrill, D.J., 2000, Cretaceous (Late Albian) coniferales of Alexander Island, Antarctica. 1: Wood taxonomy: a quantitative approach: Review of Palaeobotany and Palynology, v. 111, no. 1–2, p. 1–17, https://doi.org/10.1016/S0034-6667(00)00012-9.

Falcon-Lang, H.J., Fensome, R.A., Gibling, M.R., Malcolm, J., Fletcher, K.R., and Holleman, M., 2007, Karst-related outliers of the Cretaceous Chaswood Formation of Maritime Canada: Canadian Journal of Earth Sciences, v. 44, no. 5, p. 619–642, https://doi.org/10.1139/e06-119.

Feller, I.C., 2002, The role of herbivory by wood-boring insects in mangrove ecosystems in Belize: Oikos, v. 97, no. 2, p. 167–176, https://doi.org/10.1034/j.1600-0706.2002.970202.x.

Föllmi, K.B., 2012, Early Cretaceous life, climate and anoxia: Cretaceous Research, v. 35, p. 230–257, https://doi.org/10.1016/j.cretres.2011.12.005.

Freymueller, N.A., Moore, J.R., and Myers, C.E., 2019, An analysis of the impacts of Cretaceous oceanic anoxic events on global molluscan diversity dynamics. Paleobiology, vol. 45, no. 2, p. 280–295. https://doi.org/10.1017/pab.2019.10

Friedman, W.E., 2009, The meaning of Darwin's "abominable mystery.": American Journal of Botany, v. 96, no. 1, p. 5–21, https://doi.org/10.3732/ajb.0800150.

Garrison, J.R., Brinkman, D., Nichols, D.J., Layer,P., Burge, D., and Thayn, D., 2007, A multidisciplinary study of the Lower Cretaceous Cedar Mountain Formation, Mussentuchit Wash, Utah: A determination of the paleoenvironment and paleoecology of the *Eolambia caroljonesa* dinosaur quarry: Cretaceous Research, v. 28, no. 3, p. 461–494, https://doi.org/10.1016/j.cretres.2006.07.007.

Gee, C.T., Dayvault, R.D., Stockey, R.A., and Tidwell, W.D., 2014, Greater palaeobiodiversity in conifer seed cones in the Upper Jurassic Morrison Formation of Utah, USA: Palaeobiodiversity and Palaeoenvironments, vol. 94, no. 2, p. 363–375, https://doi.org/10.1007/s12549-014-0160-1.

Genise, J.F., and Hazeldine, P.L., 1995, A new insect trace fossil in Jurassic wood from Patagonia, Argentina: Ichnos, vol. 4, no. 1, p. 1–5, https://doi.org/10.1080/10420949509380109.

Gothan, W., 1905, Zur Anatomie lebender und fossiler Gymnospermen-Hölzer. Germany: In Vertrieb bei der Königlichen Geologischen Landesanstalt und Bergakademie.

Grossnickle, D.M., and Newham, E., 2016, Therian mammals experience an ecomorphological radiation during the Late Cretaceous and selective extinction at the K–Pg boundary: Proceedings of the Royal Society B: Biological Sciences, vol. 283, no. 1832, 20160256, https://doi.org/10.1098/rspb.2016.0256.

Guo, Q., Kato, M., and Ricklefs, R.E., 2003, Life history, diversity and distribution: A study of Japanese pteridophytes: Ecography, vol. 26, no. 2, p. 129–138, https://doi.org/10.1034/j.1600-0587.2003.03379.x.

Haq, B.U., Hardenbol, J., and Vail, P.R., 1987, Chronology of fluctuating sea levels since the Triassic: Science, vol. 235, no. 4793, p. 1156–1167, https://doi.org/10.1126/science.235.4793.1156.

Harris, E.B., and Arens, N.C., 2016, A mid-Cretaceous angiosperm-dominated macroflora from the Cedar Mountain Formation of Utah, USA: Journal of Paleontology, vol. 90, no. 4, p. 640–662, https://doi.org/10.1017/jpa.2016.44.

Hatzell, G.A., 2015, Paleoclimate implications from stable isotope analysis of sedimentary organic carbon and vertebrate fossils from the Cedar Mountain Formation, UT, U.S.A. [Masters thesis] University of Arkansas, 63 p.

Hay, W.W., and Floegel, S., 2012, New thoughts about the Cretaceous climate and oceans: Earth-Science Reviews, vol. 115, no. 4, p. 262–272, https://doi.org/10.1016/j.earscirev.2012.09.008.

Herendeen, P.S., 1991, Lauraceous wood from the mid-Cretaceous Potomac group of eastern North America: *Paraphyllanthoxylon marylandense* sp. nov.: Review of Palaeobotany and Palynology, vol. 69, no. 4, p. 277–290, https://doi.org/10.1016/0034-6667(91)90032-X.

Herendeen, P.S., Crepet, W.L., and Nixon, K.C., 1994, Fossil flowers and pollen of Lauraceae from the Upper Cretaceous of New Jersey: Plant Systematics and Evolution, vol. 189, no. 1–2, p. 29–40, https://doi.org/10.1007/BF00937576.

Ibrahim, A., 2015, Late Cretaceous conifer woods of Terlingua Ranch, Brewster County, Texas. [Masters thesis] Texas State University, 63 p.

Jenkyns, H.C., 2010, Geochemistry of oceanic anoxic events: Review. Geochemistry, Geophysics, Geosystems, vol. 11, no. 3. https://doi.org/10.1029/2009GC002788

Joeckel, R.M., Ludvigson, G.A., Möller, A., Hotton, C.L., Suarez, M.B., Suarez, C.A., Sames, B., Kirkland, J.I., and Hendrix, B., 2020, Chronostratigraphy and terrestrial palaeoclimatology of Berriasian–Hauterivian strata of the Cedar Mountain Formation, Utah, USA: Geological Society, London, Special Publications, vol. 498, no. 1, p. 75–100, https://doi.org/10.1144/SP498-2018-133.

Joeckel, R.M., Suarez, C.A., McLean, N.M., Möller, A., Ludvigson, G.A., Suarez, M.B., Kirkland, J.I., Andrew, J., Kiessling, S., and Hatzell, G.A., 2023, Berriasian–Valanginian geochronology and carbon-isotope stratigraphy of the Yellow Cat Member, Cedar Mountain Formation, Eastern Utah, USA: Geosciences, vol. 13, no. 2, 32, https://doi.org/10.3390/geosciences13020032.

Jud, N.A., Wheeler, E.A., Rothwell, G.W., and Stockey, R.A., 2017, Angiosperm wood from the Upper Cretaceous (Coniacian) of British Columbia, Canada: IAWA Journal, vol. 38, no. 2, p. 141-161, doi: https://doi.org/10.1163/22941932-20170164.

Karmakar, R., Das, I., Dutta, D., and Rakshit, A., 2016, Potential effects of climate change on soil properties: A review. Science International, vol. 4, no. 2, p. 51–73. https://doi.org/10.17311/sciintl.2016.51.73

Kidder, D.L., and Worsley, T.R., 2010, Phanerozoic Large Igneous Provinces (LIPs), HEATT (Haline Euxinic Acidic Thermal Transgression) episodes, and mass extinctions: Palaeogeography, Palaeoclimatology, Palaeoecology, vol. 295, no. 1–2, p. 162–191, https://doi.org/10.1016/j.palaeo.2010.05.036.

Kim, K., Jeong, E.K., Suzuki, M., Huh, M., and Paik, I.S., 2002, Some coniferous fossil woods from the Cretaceous of Korea: Geosciences Journal, vol. 6, no. 2, p. 131–140, https://doi.org/10.1007/BF03028284.

Kim, K., Suzuki, M., and Oh, C., 2005, Re-examination of Prof. Shimakura's coniferous fossil wood microscope slides deposited in Tohoku University Museum: Bulletin of the Tohoku University Museum, vol. 4, p. 17-72, http://hdl.handle.net/10097/54396.

Kirkland, J., Britt, B., Burge, D., Carpenter, K., Cifelli, R., Decourten, F., Hasiotis, S. and Lawton, T., 1997, Lower to middle Cretaceous dinosaur faunas of the central Colorado Plateau: a key to understanding 35 million years of tectonics, sedimentology, evolution and biogeography: Brigham Young University Geology Studies, vol. 42, p. 69-103.

Kirkland, J.I., Suarez, M., Suarez, C., and Hunt-Foster, R., 2016, The Lower Cretaceous in east-central Utah—the Cedar Mountain Formation and its bounding strata: Geology of the Intermountain West, vol. 3, p. 101–228.

Knoll, A.H., 1986, Patterns of change in plant communities through geologic time. p. 126–141. In Diamond, J., and Case, T. J. (eds.), Community Ecology. Harper and Row; New York.

Kohn, M.J., 2010, Carbon isotope compositions of terrestrial C3 plants as indicators of (paleo)ecology and (paleo)climate: PNAS, v. 107, no. 46, p. 19691–19695.

Leckie, R.M., Bralower, T.J., and Cashman, R., 2002, Oceanic anoxic events and plankton evolution: Biotic response to tectonic forcing during the mid-Cretaceous: Oceanic anoxic events and plankton evolution. Paleoceanography, vol. 17, no. 3, p. 13–29. https://doi.org/10.1029/2001PA000623

Lidgard, S., and Crane, P. 1988. Quantitative analyses of the early angiosperm radiation: Nature, vol. 331, p. 344–346, https://doi.org/10.1038/331344a0.

Liu, L., Zhang, J., Rheindt, F.E., Lei, F., Qu, Y., Wang, Y., Zhang, Y., Sullivan, C., Nie, W., Wang, J., Yang, F., Chen, J., Edwards, S.V., Meng, J., and Wu, S., 2017, Genomic evidence reveals a radiation of placental mammals uninterrupted by the K-Pg boundary: Proceedings of the National Academy of Sciences, vol. 114, no. 35, https://doi.org/10.1073/pnas.1616744114.

Lloyd, G.T., Davis, K.E., Pisani, D., Tarver, J.E., Ruta, M., Sakamoto, M., Hone, D.W.E., Jennings, R., and Benton, M.J., 2008, Dinosaurs and the Cretaceous Terrestrial Revolution: Proceedings of the Royal Society B: Biological Sciences, vol. 275, no. 1650, p. 2483–2490, https://doi.org/10.1098/rspb.2008.0715.

Ludvigson, G. A., Joeckel, R. M., Murphy, L. R., Stockli, D. F., González, L. A., Suarez, C. A., Kirkland, J. I., and Al-Suwaidi, A., 2015, The emerging terrestrial record of Aptian-Albian global change. Cretaceous Research, vol. 56, p. 1–24. https://doi.org/10.1016/j.cretres.2014.11.008

Ludvigson, G.A., Joeckel, R.M., Gonzalez, L.A., Gulbranson, E.L., Rasbury, E.T., Hunt, G.J., Kirkland, J.I., and Madsen, S., 2010, Correlation of Aptian-Albian carbon isotope excursions in continental strata of the Cretaceous Foreland Basin, Eastern Utah, U.S.A.: Journal of Sedimentary Research, vol. 80, no. 11, p. 955–974, https://doi.org/10.2110/jsr.2010.086.

Lupia, R., Lidgard, S., and Crane, P. R., 1999, Comparing palynological abundance and diversity: Implications for biotic replacement during the Cretaceous angiosperm radiation. Paleobiology, vol. 25, no. 3, p. 305–340. https://doi.org/10.1017/S009483730002131X

Mannion, P. D., and Upchurch, P., 2011, A re-evaluation of the 'mid-Cretaceous sauropod hiatus' and the impact of uneven sampling of the fossil record on patterns of regional dinosaur extinction. Palaeogeography, Palaeoclimatology, Palaeoecology, vol. 299, no. 3-4, p. 529–540. https://doi.org/10.1016/j.palaeo.2010.12.003

Meijer, J. J. F., 2000, Fossil woods from the Late Cretaceous Aachen Formation. Review of Palaeobotany and Palynology, vol. 112, no. 4, p. 297–336. https://doi.org/10.1016/S0034-6667(00)00007-5

Mikuláš, R., Milàn, J., Genise, J.F., Bertling, M., and Bromley, R.G., 2020, An insect boring in an Early Cretaceous wood from Bornholm, Denmark, Ichnos, vol. 27, no. 3, p. 284-289. DOI: 10.1080/10420940.2020.1744587

Naeher Stephens, T.M. (2005) Palynological Analysis of vertebrate habitats: Cedar Mountyain Fm. (Albian-Cenomanian) of Utah. [Masters thesis] University of Oklahoma, 156 p.

Nagalingum, N. S., Drinnan, A. N., Lupia, R., and McLoughlin, S., 2002, Fern spore diversity and abundance in Australia during the Cretaceous. Review of Palaeobotany and Palynology, vol. 119, no. 1-2, p. 69–92. https://doi.org/10.1016/S0034-6667(01)00130-0

Nagy, N.E., Franceschi, V.R., Solheim, H., Krekling, T., and Christiansen, E., 2000, Wound-induced traumatic resin duct development in stems of Norway spruce (Pinaceae): anatomy and cytochemical traits. American Journal of Botany, vol. 87, p. 302-313. https://doi.org/10.2307/2656626

Nishida, H., 1986, 818. A new species of Tempskya from Japan, Journal of the Palaeontological Society of Japan, New Edition, 1986(143), 435-446, https://doi.org/10.14825/prpsj1951.1986.143_435

Nishida, M., and Nishida, H., 1986, Structure and affinities of the petrified plants from the cretaceous of Northern Japan and Saghalien III: Petrified plants from the Upper Cretaceous of Saghalien. The Botanical Magazine Tokyo, vol. 99, no. 2, p. 191–204. https://doi.org/10.1007/BF02488820

Noss, R., 2000, The redwood forest: History, ecology, and conservation of the coast redwoods. Island Press. ISBN 978-1559637268. OCLC 925183647.

Novacek, M. J., 1999, 100 million years of land vertebrate evolution: The Cretaceous-Early Tertiary transition. Annals of the Missouri Botanical Garden, vol. 86, no. 2. https://doi.org/10.2307/2666178

Oh, C., Kim, K., Paik, I.-S., and Lim, J.-D., 2011, Cretaceous conifer woods of Korea: Occurrences and palaeobiological implications. Review of Palaeobotany and Palynology, vol. 164, no. 1-2, p. 67–83. https://doi.org/10.1016/j.revpalbo.2010.11.007

Palakit, K., Siripattanadilok, S., and Duangsathaporn, K., 2012, False ring occurrences and their identification in Teak (*Tectona grandis*) in North-eastern Thailand. Journal of Tropical Forest Science, vol. 24, no. 3, p. 387-398, https://www.jstor.org/stable/23617123

Parameswaran, N., and Gomes, A. V., 1981, Fine structural aspects of helical thickenings and pits in vessels of *Ligustrum Lucidum* Ait. (Oleaceae), IAWA Journal, vol. 2, no. 4, p. 179-185. doi: https://doi.org/10.1163/22941932-90000728

Penhallow, D. P., 1908, Report on a collection of fossil woods from the Cretaceous of Alberta. The Ottawa Naturalist, 22(4), 81-88, https://doi.org/10.5962/bhl.title.65444

Philippe, M., and Bamford, M. K., 2008, A key to morphogenera used for Mesozoic conifer-like woods. Review of Palaeobotany and Palynology, vol. 148, no. 2-4, p. 184–207. https://doi.org/10.1016/j.revpalbo.2007.09.004

Quan, C., Sun, C., Sun, Y., and Sun, G., 2009, High resolution estimates of paleo-CO_2 levels through the Campanian (Late Cretaceous) based on Ginkgo cuticles. Cretaceous Research, vol. 30, no. 2, p. 424-428. https://doi.org/10.1016/j.cretres.2008.08.004

Ramanujam, C. G. K., 1972, Fossil coniferous woods from the Oldman Formation (Upper Cretaceous) of Alberta. Canadian Journal of Botany, vol. 50, no. 3, p. 595–602. https://doi.org/10.1139/b72-073

Ramanujam, C. G. K., and Stewart, W. N., 1969b, Fossil woods of Taxodiaceae from the Edmonton Formation (Upper Cretaceous) of Alberta. Canadian Journal of Botany, vol. 47, no. 1, p. 115-124. https://doi.org/10.1139/b69-015

Ramanujam, C. G. K., and Stewart, W. N., 1969c, Nomenclatural changes for *Taxodioxylon antiquum* Ramanujam & Stewart and *T. antiquum* Prakash. Canadian Journal of Botany, vol. 47, no. 8, p. 1333-1334. https://doi.org/10.1139/b69-189

Richter, H.G., Grosser, D., Heinz, I., and Gasson, P.E., 2004, IAWA list of microscopic features for softwood identification. IAWA Journal, vol. 25, p. 1-70.

Ríos-Santos, C., and Cevallos-Ferriz, S. R. S., 2019, Upper Jurassic, Upper Cretaceous and Palaeocene conifer woods from Mexico. Earth and Environmental Science Transactions of the Royal Society of Edinburgh, vol. 108, no. 4, p. 399-418. https://doi.org/10.1017/S1755691018000245

Robertson, C.H., 2019, stable isotope geochemistry and paleohydrology of the Poison Strip Sandstone, Early Cretaceous, Eastern Utah. [Masters thesis] University of Kansas, 37 p.

Román-Jordán, E., Esteban, L. G., de Palacios, P., and Fernández, F. G., 2017, Comparative wood anatomy of the Cupressaceae and correspondence with phylogeny, with special reference to the monotypic taxa. Plant Systematics and Evolution, vol. 303, no. 2, p. 203–219. https://doi.org/10.1007/s00606-016-1364-9

Shimakura, M., 1937, Studies on fossil woods from Japan and adjacent lands contribution II: The Cretaceous woods from Japan, Saghalien, and Manchoukuo. Science reports of the Tohoku Imperial University. 2nd series, Geology, vol. 19, no. 1, p. 1-103.

Shimakura, M., 1940, 98. On the occurrence of *Taxodioxylon albertense* (Penhallow) in the Senonian of Karahuto (Japanese Saghalien). The Journal of the Geological Society of Japan, vol. 47, no. 556, p. 45-48. https://doi.org/10.5575/geosoc.47.45

Simonin, K. A., and Roddy, A. B., 2018, Genome downsizing, physiological novelty, and the global dominance of flowering plants. PLOS Biology, vol. 16, no.1, e2003706. https://doi.org/10.1371/journal.pbio.2003706

Skelton, J., Jusino, M.A., Carlson, P.S., Smith, K., Banik, M.T., Lindner, D.L., Palmer, J.M., and Hulcr, J., 2019, Relationships among wood-boring beetles, fungi, and the decomposition of forest biomass. Molecular Ecology, vol. 28, no. 22, p. 4971–4986. https://doi.org/10.1111/mec.15263

Sorscher, A. A. R., 2022, An herbivorous dinosaur coprolite from the Lower Cretaceous Ruby Ranch Member of the Cedar Mountain Formation, Utah, USA: organic contents, taphonomy, and diagenesis. [Masters thesis] University of Colorado, 66 p.

Srivastava, S.K., 1968, Eight species of Mancicorpus from the Edmonton Formation (Maestrichtian), Alberta, Canada. Canadian Journal of Botany, vol. 46, no. 12, p. 1485-1490. https://doi.org/10.1139/b68-205

Suarez, M.B., Knight, J.A., Godet, A., Ludvigson, G.A., Snell, K.E., Murphy, L., and Kirkland, J.I., 2021, Multiproxy strategy for determining palaeoclimate parameters in the Ruby Ranch Member of the Cedar Mountain Formation. Geological Society, London, Special Publications, vol. 507, no. 1, p. 313–334. https://doi.org/10.1144/SP507-2020-85

Suarez, M.B., Suarez, C.A., Al-Suwaidi, A.H., Hatzell, G., Kirkland, J.I., Salazar-Verdin, J., Ludvigson, G.A., and Joeckel, R.M., 2017, Terrestrial carbon isotope chemostratigraphy in the Yellow Cat Member of the Cedar Mountain Formation. In Terrestrial Depositional Systems (pp. 303–336). Elsevier. https://doi.org/10.1016/B978-0-12-803243-5.00008-X

Tennant, J. P., Mannion, P. D., Upchurch, P., Sutton, M. D., and Price, G. D., 2017, Biotic and environmental dynamics through the Late Jurassic-Early Cretaceous transition: Evidence for protracted faunal and ecological turnover: Jurassic-Cretaceous biotic and abiotic dynamics. Biological Reviews, vol. 92, no. 2, p. 776–814. https://doi.org/10.1111/brv.12255

Thayn, G. F., and Tidwell, W. D., 1984, Flora of the Lower Cretaceous Cedar Mountain Formation of Utah and Colorado, part II. *Mesembrioxylon stokesi*. The Great Basin Naturalist, vol. 44, no. 2, p. 257–262. http://www.jstor.org/stable/41712069

Thayn, G. F., Tidwell, W. D., and Stokes, W. L., 1985, Flora of the Lower Cretaceous Cedar Mountain Formation of Utah and Colorado. Part III: *Icacinoxylon pittiense* n. sp. American Journal of Botany, vol. 72, no. 2, p. 175–180. https://doi.org/10.2307/2443544

Thayne, G. F., Tidwell, W. D., and Stokes, W. L., 1983, Flora of the Lower Cretaceous Cedar Mountain Formation of Utah and Colorado, part I. *Paraphyllanthoxylon utahense*. The Great Basin Naturalist, vol. 43, no. 3, p. 394–402. http://www.jstor.org/stable/41711990

Therrell, M. D., Elliott, E. A., Meko, M. D., Bregy, J. C., Tucker, C. S., Harley, G. L., Maxwell, J. T., and Tootle, G. A., 2020, Streamflow variability indicated by false rings in Bald Cypress (*Taxodium distichum* (L.) Rich.). Forests, vol. 11, no. 10. https://doi.org/10.3390/f11101100

Tian, N., Zhu, Z., Wang, Y., Philippe, M., Chou, C., and Xie, A., 2018 *Sequoioxylon zhangii* sp. nov. (Sequoioideae, Cupressaceae s.l.), a new coniferous wood from the Upper Cretaceous in Heilongjiang Province, Northeast China. Review of Palaeobotany and Palynology, vol. 257, p. 85-94.

Tidwell, W. D., and Hebbert, N., 1992, Species of the Cretaceous tree fern Tempskya from Utah. International Journal of Plant Sciences, vol. 153, no. 3, part 1, p. 513–528. https://doi.org/10.1086/297057

Tidwell, W. D., and Thayn, G. F., 1985, Flora of the Lower Cretaceous Cedar Mountain Formation of Utah and Colorado, Part IV. *Palaeopiceoxylon thinosus* (Protopinaceae). The Southwestern Naturalist, vol. 30, no. 4, p. 525. https://doi.org/10.2307/3671046

Tidwell, W.D., Britt, B.B., and Tidwell, L.S., 2007, A review of the Cretaceous floras of East-Central Utah and Western Colorado. In, Willis, G.C., Hylland, M.D., Clark, D.L., and Chidsey, T.C., Jr., editors, Central Utah - diverse geology of a dynamic landscape. Utah Geological Association Publication 36, p. 467-482.

Torrey, R. E., 1923, The comparative anatomy and phylogeny of the Coniferales. Memoirs of the Boston Society of Natural History, vol. 6, no. 2, p. 39-106

Traverse, A., 2004, (1643) Proposal to conserve the fossil pollen morphogeneric name *Classopollis* against *Corollina* and *Circulina*. TAXON, vol. 53, no. 3, p. 847–848. https://doi.org/10.2307/4135468

Traverse, A., 2007, Paleopalynology: Second Edition. Netherlands: Springer.

Tschudy, R.H., Tschudy, B.D., and Craig, L.C., 1984, Palynological evaluation of Cedar Mountain and Burro Canyon formations, Colorado Plateau (Report No. 1281; Professional Paper). USGS Publications Warehouse. https://doi.org/10.3133/pp1281

Tucker, R.T., Suarez, C.A., Makovicky, P.J., and Zanno, L.E., 2022, Paralic sedimentology of the Mussentuchit Member coastal plain, Cedar Mountain Formation, central Utah, U.S.A. Journal of Sedimentary Research, vol. 92(6), 546–569. https://doi.org/10.2110/jsr.2021.028

United States Department of Agriculture (2011) Introduction to Wood Borers. https://www.fs.usda.gov/Internet/FSE_DOCUMENTS/stelprdb5347203.pdf

Velitzelos, E., and Zouros, N., 2006, The petrified forest of Lesvos, Topio publications, Athens, 160 pp.

Wang, Y., Huang, C., Sun, B., Quan, C., Wu, J., and Lin, Z., 2014, Paleo-CO_2 variation trends and the Cretaceous greenhouse climate. Earth-Science Reviews, vol. 129, p. 136–147. https://doi.org/10.1016/j.earscirev.2013.11.001

Wheeler, E.A., 2011, InsideWood - a web resource for hardwood anatomy. IAWA Journal, vol. 32, no. 2, p. 199-211.

Wheeler, E.A., Baas, P., and Gasson, P.E., 1989, IAWA list of microscopic features for hardwood identification: With an appendix on non-anatomical information.

Wing, S. L., and Tiffney, B. H., 1987, The reciprocal interaction of angiosperm evolution and tetrapod herbivory. Review of Palaeobotany and Palynology, vol. 50, no. 1-2, p. 179–210. https://doi.org/10.1016/0034-6667(87)90045-5

Yang, Z.-Y., Ran, J.-H., and Wang, X.-Q., 2012, Three genome-based phylogeny of Cupressaceae s.l.: Further evidence for the evolution of gymnosperms and Southern Hemisphere biogeography. Molecular Phylogenetics and Evolution, vol. 64, no. 3, p. 452-470. https://doi.org/10.1016/j.ympev.2012.05.004

Young, R. G., 1960, Dakota group of Colorado plateau. AAPG Bulletin, vol. 44, no. 2, p. 156-194.

Zhang, W., Li, Y., Xu, T., Cheng, H., Zheng, Y., and Xiong, P., 2009, Long-term variations of CO_2 trapped in different mechanisms in deep saline formations: A case study of the Songliao Basin, China, vol. 3, no. 2, p. 161–180. doi:10.1016/j.ijggc.2008.07.007

Zouros, N., 2021, The Miocene petrified forest of Lesvos, Greece: Research and geoconservation activities. Geoconservation Research, vol. 4, no. 2. https://doi.org/10.30486/gcr.2021.1927340.1090